Table of Contents

1. General Information and Materials

^{1}H nuclear magnetic resonance (NMR), ^{19}F NMR and ^{13}C NMR spectra were measured on the Agilent MR 400 and Bruker MR 500 spectrometer, and were calibrated using residual undeuterated solvent ($CHCl_3$ at 7.26 ppm ^{1}H NMR; $CDCl_3$ at 77.0 ppm ^{13}C NMR; $CFCl_3$ as an external standard and low field is positive ^{19}F NMR). Chemical shifts (δ) are reported in ppm and coupling constants (*J*) are in Hertz (Hz). The following abbreviations were used to explain the multiplicities: s = singlet, d = doublet, t = triplet, q = quartet, m = multiplet, br = broad. High Resolution Mass spectral data were recorded on Waters GC-TOF Premier spectrometer in EI mode, Agilent Technologies 6224 TOF LC MS spectrometer in ESI mode. Elemental analysis (EA) was performed by an Elementar Vario EL cube. Electron paramagnetic resonance (EPR) spectra were conducted at 298 K on a Bruker E500 EPR spectrometer. UV-Vis spectra were measured using a Varian Cary 100 Scan spectrophotometer with a slit width of 1.0 nm and a wavelength range of 200-400 nm.

All reagents were used as received from commercial sources or prepared as described in the literature. Graphite felt electrodes (thickness: 7 mm and 5.5 mm) were supplied by Rensheng Graphite Felt Co., Ltd. (Jiangyou, China). Cation-exchange membrane (NEPEM 1135, thickness: 80 μm) was supplied by Suzhou Thinkre New Material Co., Ltd. (Jiangsu, China). Graphite bipolar plates (thickness: 1 mm) were supplied by ResinDa Co., Ltd. (Foshan, China). 4-Hydroxy-2,2,6,6-tetramethylpiperidin-1-oxyl (**4-HO-TEMPO**, 99%), and zinc chloride ($ZnCl_2$, 99%) were purchased from Meryer Co., Ltd. (Shanghai, China). Ammonium chloride (NH_4Cl, 99%) was purchased from Shanghai Dahe Chemicals Co., Ltd. (Shanghai, China).

2. Synthesis of DFTEMPO and NFTEMPO

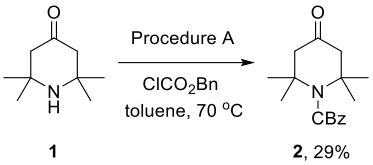

Procedure A: To a 1 L schlenk flask was added 2,2,6,6-tetramethyl-4-oxopiperidine (77.60 g, 500.0 mmol, 1.0 equiv). The reaction flask was charged with toluene (400 mL) and cooled to 0 °C in an ice-salt bath, followed by the slow addition of benzyl chloroformate (85.30 g, 500.0 mmol, 1.0 equiv). After connecting to a tail gas treatment unit containing sodium hydroxide solution, the reaction flask was pre-stirred at room temperature for 5 min, and then placed in a pre-heated oil bath (70 °C) and stirred for 48 h. Then, the reaction solution was cooled to room temperature, diluted with of ethyl acetate (200 mL) and washed with 0.5 M HCl solution (200 mL*3), saturated $NaHCO_3$ solution (200 mL*3), and brine (400 mL) in sequence. The organic layer was collected, dried over anhydrous sodium sulfate, filtered and concentrated under reduced pressure. Finally, the residue was purified by silica gel flash column chromatography (ethyl acetate: hexane=1:20) to obtain the desired product benzyl 2,2,6,6-tetramethyl-4-oxopiperidine-1-carboxylate (**2**, 41.82 g, 28.9%) as a white crystal. ^{1}H NMR (400 MHz, $CDCl_3$) δ 7.40 – 7.29 (m, 5H), 5.15 (s, 2H), 2.57 (s, 4H), 1.47 (s, 12H). ^{13}C NMR (126 MHz, $CDCl_3$) δ 207.9, 156.3, 136.2, 128.4, 128.2, 128.0, 66.6, 56.5, 53.2, 30.0. MS (ESI): m/z (%) 312 ($[M+Na]^+$). HRMS (ESI) m/z: ($[M+Na]^+$) Calcd. for $C_{17}H_{23}NO_3Na$: 312.1570; Found: 312.1576.

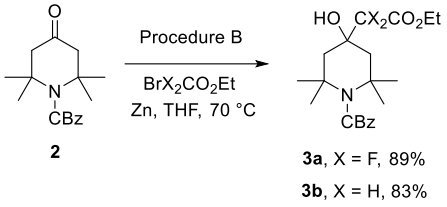

Procedure B: To a three-necked flask were added **2** (for **X = F**, 40.38 g, 140.0 mmol, 1.0 equiv; for **X = H**, 1.45 g, 5.0 mmol, 1.0 equiv) and activated zinc powder (for **X = F**, 18.31 g, 280.0 mmol, 2.0 equiv; for **X = H**, 0.65 g, 10.0 mmol, 2.0 equiv). The three-necked flask was charged with tetrahydrofuran (THF) and heated to 75 °C, followed by the slow addition of $BrCX_2CO_2Et$ (for **X = F**, 56.83 g, 280.0 mmol, 2.0 equiv; for **X = H**, 1.67 g, 10.0 mmol, 2.0 equiv). Then the reaction solution refluxed at 75 °C for 6 h. Upon completion, the reaction solution was cooled to room temperature, quenched with water, and washed with 0.5 M HCl solution (200 mL*3), saturated $NaHCO_3$ solution

(200 mL*3), and brine (400 mL) in sequence. The organic layer was collected, dried over anhydrous sodium sulfate, filtered and concentrated. The residue was purified with flash chromatography to afford the product.

Benzyl 4-(2-ethoxy-1,1-difluoro-2-oxoethyl)-4-hydroxy-2,2,6,6-tetramethylpiperidine-1-carboxylate (**3a**). The product (51.80 g, 89% yield) was purified with silica gel chromatography (petroleum ether/ ethyl acetate = 10:1) as a white solid. ^{1}H NMR (400 MHz, $CDCl_3$) δ 7.40 – 7.28 (m, 5H), 5.13 (s, 2H), 4.36 (q, *J* = 7.2 Hz, 2H), 2.58 (s, 1H), 2.40 (d, *J* = 15.5 Hz, 2H), 1.87 (d, *J* = 15.5 Hz, 2H), 1.53 (s, 6H), 1.45 (s, 6H), 1.36 (t, *J* = 7.2 Hz, 3H). ^{19}F NMR (376 MHz, $CDCl_3$) δ -117.8 (s, 2F). ^{13}C NMR (126 MHz, $CDCl_3$) δ 163.5 (t, *J* = 32.3 Hz), 156.4, 136.4, 128.3, 128.1, 127.8, 115.0 (t, *J* = 260.8 Hz), 71.5 (t, *J* = 24.8 Hz), 66.4, 63.0, 55.0, 43.9, 30.4, 13.8. MS (ESI): m/z (%) 436 ($[M+Na]^+$). HRMS (ESI) m/z: ($[M+Na]^+$) Calcd. for $C_{21}H_{29}NO_5F_2Na$: 436.1906; Found: 436.1900.

Benzyl 4-(2-ethoxy-2-oxoethyl)-4-hydroxy-2,2,6,6-tetramethylpiperidine-1-carboxylate (**3b**). The product (1.56 g, 83% yield) was purified with silica gel chromatography (petroleum ether/ ethyl acetate = 10:1) as a white solid. ^{1}H NMR (400 MHz, $CDCl_3$) δ 7.42 – 7.25 (m, 5H), 5.12 (s, 2H), 4.19 (q, *J* = 7.2 Hz, 2H), 3.93 (s, 1H), 2.58 (s, 1H), 2.07 (d, *J* = 15.0 Hz, 2H), 1.90 (d, *J* = 15.0 Hz, 2H), 1.51 (s, 6H), 1.41 (s, 6H), 1.29 (t, *J* = 7.2 Hz, 3H). ^{13}C NMR (126 MHz, $CDCl_3$) δ 172.5, 156.4, 136.6, 128.3, 128.0, 127.7, 67.3, 66.2, 60.8, 55.4, 49.8, 47.9, 30.2, 29.8, 14.0. MS (ESI): m/z (%) 400 ($[M+Na]^+$). HRMS (ESI) m/z: ($[M+Na]^+$) Calcd. for $C_{21}H_{31}NO_5Na$: 400.2091; Found: 400.2094.

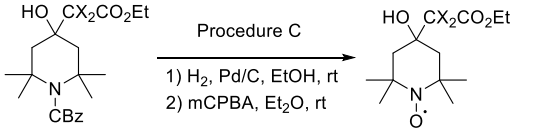

3a, X = F — **4a**, X = F, 82% (2 steps)

3b, X = H — **4b**, X = H, 84% (2 steps)

Procedure C: 1) To an autoclave cannula were added **3** (for **X = F**, 30.00 g, 72.5 mmol, 1.0 equiv; for **X = H**, 5.36 g, 14.2 mmol, 1.0 equiv), Pd/C (for **X = F**, 1.50 g, 1.5 mmol, 2 mol%; for **X = H**, 0.64 g, 0.3 mmol, 2 mol%), and ethanol. The autoclave was sealed, and the internal gas is replaced with hydrogen (60 atm). Then the autoclave was stirred at 25 °C for 24 h. After the starting material was completely consumed by ^{19}F NMR, the reaction solution was filtered, and concentrated under reduced pressure to obtain the crude product, which can be used for the next step without further purification.

Ethyl 2-(4-hydroxy-2,2,6,6-tetramethylpiperidin-4-yl)-2,2-difluoroacetate (**F3**). The product

(20.59 g, quant. yield) was a white solid, ^{1}H NMR (500 MHz, $CDCl_3$) δ 4.36 (q, *J* = 7.0 Hz, 2H), 2.53 (br, 1H), 1.74 (d, *J* = 14.0 Hz, 2H), 1.48 (d, *J* = 14.0 Hz, 2H), 1.38 (s, 6H), 1.36 (t, *J* = 7.5 Hz, 3H), 1.17 (s, 6H). ^{19}F NMR (376 MHz, $CDCl_3$) δ -119.8 (s, 2F). ^{13}C NMR (126 MHz, $CDCl_3$) δ 163.6 (t, *J* = 32.3 Hz), 115.1 (t, *J* = 260.4 Hz), 75.7 (t, *J* = 22.8 Hz), 63.0, 49.6, 39.2, 35.6, 30.1, 14.0. MS (ESI): m/z (%) 280 ($[M+H]^+$). HRMS (ESI) m/z: ($[M+H]^+$) Calcd. for $C_{13}H_{24}NO_3F_2$: 280.1719; Found: 280.1717.

Ethyl 2-(4-hydroxy-2,2,6,6-tetramethylpiperidin-4-yl)-acetate (**H3**). The product (3.34 g, 97% yield) was a white solid. ^{1}H NMR (400 MHz, $CDCl_3$) δ 4.14 (q, *J* = 5.6 Hz, 2H), 3.63 (s, 1H), 2.35 (s, 2H), 1.75 (d, *J* = 13.6 Hz, 2H), 1.37 (s, 6H), 1.24 (t, *J* = 7.2 Hz, 3H), 1.11 (d, *J* = 13.6 Hz, 2H), 1.07 (s, 6H). ^{13}C NMR (126 MHz, $CDCl_3$) δ 172.8, 71.0, 60.6, 50.0, 48.0, 46.8, 35.6, 29.5, 14.1. MS (ESI): m/z (%) 244 ($[M+H]^+$). HRMS (ESI) m/z: ($[M+H]^+$) Calcd. for $C_{13}H_{26}NO_3$: 244.1907; Found: 244.1906.

2) To a round bottom flask were added **F3** or **H3** (for **X = F**, 7.90 g, 28.3 mmol, 1.0 equiv; for **X = H**, 3.34 g, 13.7 mmol, 1.0 equiv) and ether (200 ml). The reaction mixture was cooled to 0 °C in an ice-salt bath before 3-chloroperoxybenzoic acid (for **X = F**, 9.77 g, 56.6 mmol, 2.0 equiv; for **X = H**, 5.57 g, 27.5 mmol, 2.0 equiv) was added in batches. The reaction mixture was stirred at room temperature for 12 h, and then washed with saturated $NaHCO_3$ solution (100 mL*3). The organic layer was collected, dried over anhydrous sodium sulfate, filtered, and concentrated. The residual was purified by flash column chromatography to afford the product.

Ethyl 2-(4-hydroxy-2,2,6,6-tetramethylpiperidin-1-oxyl-4-yl)-2,2-difluoroacetate (**4a**). The product (6.84 g, 82%) was purified with silica gel chromatography (petroleum ether/ ethyl acetate = 10:1) as an orange solid. (***NOTE:*** The synthesized **4a** was reduced by phenylhydrazine for NMR test.) ^{1}H NMR (400 MHz, $CDCl_3$) δ 4.34 (q, *J* = 7.2 Hz, 2H), 1.88 (d, *J* = 13.6 Hz, 2H), 1.80 (d, *J* = 13.6 Hz, 2H), 1.36 (s, 6H), 1.34 (t, *J* = 7.2 Hz, 3H), 1.21 (s, 6H). ^{19}F NMR (376 MHz, $CDCl_3$) δ -118.9 (s, 2F). ^{13}C NMR (126 MHz, $CDCl_3$) δ 163.5 (t, *J* = 32.4 Hz), 115.0 (t, *J* = 260.8 Hz), 74.0 (t, *J* = 23.1 Hz), 63.1, 58.0, 41.2, 32.9, 21.0, 13.9. MS (ESI): m/z (%) 317 ($[M+Na]^+$). HRMS (ESI) m/z: ($[M+Na]^+$) Calcd. for $C_{13}H_{22}NO_4F_2Na$: 317.1409; Found: 317.1414.

Ethyl 2-(4-hydroxy-2,2,6,6-tetramethylpiperidin-1-oxyl-4-yl)-acetate (**4b**). The product (3.07 g, 87% yield) was purified with silica gel chromatography (petroleum ether/ ethyl acetate = 10:1) as a light orange solid. (***NOTE***: The synthesized **4b** was reduced by phenylhydrazine for NMR test.) ^{1}H NMR (500 MHz, $CDCl_3$) δ 4.18 (q, *J* = 7.0 Hz, 2H), 2.37 (s, 2H), 1.86 (d, *J* = 13.6 Hz, 2H), 1.57 (d, *J* = 13.6 Hz, 2H), 1.41 (s, 6H), 1.28 (t, *J* = 7.0 Hz, 3H), 1.19 (s, 6H). ^{13}C NMR (126 MHz, $CDCl_3$) δ 172.9, 69.7, 60.6, 48.4, 47.4, 32.8, 20.4, 14.1. MS (ESI): m/z (%) 281 ([M+Na]$^+$). HRMS (ESI) m/z: ([M+Na]$^+$) Calcd. for $C_{13}H_{24}NO_4Na$: 281.1598; Found: 281.1596.

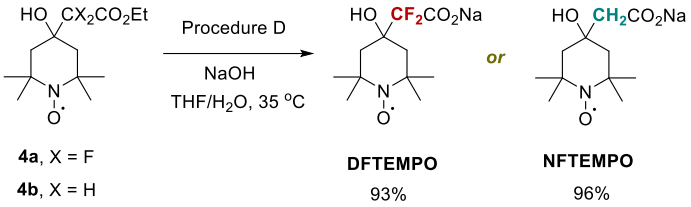

Procedure D: To a round bottom flask were added **4** (for **X = F**, 13.61 g, 46.2 mmol, 1.0 equiv; for **X = H**, 4.89 g, 18.9 mmol, 1.0 equiv), THF (200 mL), and aqueous solution (20 mL) of NaOH (for **X = F**, 1.850 g, 46.2 mmol, 1.0 equiv; for **X = H**, 0.757 g, 18.9 mmol, 1.0 equiv). The reaction mixture was stirred at 35°C for 24 h. Then the reaction mixture was concentrated and redissolved in water (50 mL). The aqueous layer was washed with dichloromethane (DCM, 100 mL*3), then concentrated and lyophilized to provide the product.

Sodium 2-(4-hydroxy-2,2,6,6-tetramethylpiperidin-1-oxyl-4-yl)-2,2-difluoroacetate dihydrate (**DFTEMPO·2H$_2$O**). The product (13.88 g, 93% yield) was an orange solid. (***NOTE***: The **DFTEMPO** was reduced by phenylhydrazine for NMR test.) ^{1}H NMR (400 MHz, D_2O) δ 1.89 (s, 4H), 1.35 (s, 6H), 1.17 (s, 6H). ^{19}F NMR (376 MHz, D_2O) δ -114.6 (s, 2F). MS (ESI): m/z (%) 265 ([M-Na]$^-$). HRMS (ESI) m/z: ([M-Na]$^-$) Calcd. for $C_{11}H_{17}NO_4F_2$: 265.1131; Found: 265.1129. Elemental analysis calcd. (%) for $C_{11}H_{21}NO_6F_2Na$: C 40.74, H 6.53, N 4.32. Found: C 40.63, H 6.47, N 4.26.

Sodium 2-(4-hydroxy-2,2,6,6-tetramethylpiperidin-1-oxyl-4-yl)-acetate tetrahydrate (**NFTEMPO·4H$_2$O**). The product (4.61 g, 96% yield) was a light orange solid. (***NOTE***: The **NFTEMPO** was reduced by phenylhydrazine for NMR test.) ^{1}H NMR (500 MHz, D_2O) 2.27 (s, 2H), 1.96 (d, *J* = 13.8 Hz, 2H), 1.73 (d, *J* = 13.8 Hz, 2H), 1.44 (s, 6H), 1.23 (s, 6H). MS (ESI): m/z (%) 229 ([M-Na]$^-$). HRMS (ESI) m/z: ([M-Na]$^-$) Calcd. for $C_{11}H_{19}NO_4$: 229.1320; Found: 229.1318. Elemental analysis calcd. (%) for $C_{11}H_{27}NO_8Na$: C 40.74, H 8.39, N 4.32. Found: C 41.57, H 8.47, N 4.28.

3. Figures and Tables

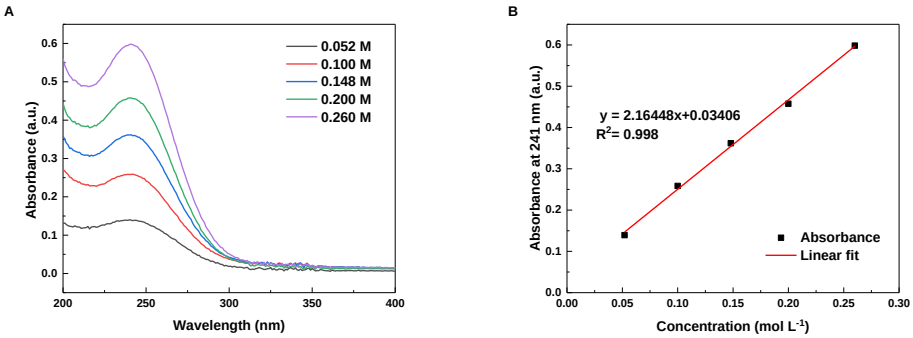

Fig. S1. UV-Vis spectra for determination of the absorbance-concentration curve of **DFTEMPO**. (**A**) UV-Vis spectra of **DFTEMPO** aqueous solutions with different concentrations. (**B**) The corresponding absorbance at 241 nm versus the concentration of **DFTEMPO** aqueous solution.

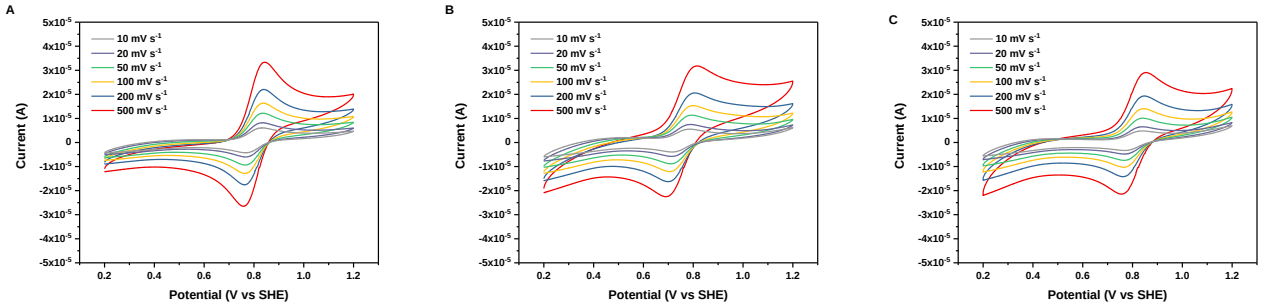

Fig. S2. CV curves of (**A**) 1 mM **4-HO-TEMPO** in 1 M NaCl solution, (**B**) 1 mM **NFTEMPO** in 1 M NaCl solution, and (**C**) 1 mM **DFTEMPO** in 1 M NaCl solution at varied scan rates from 5 to 500 mV s^{-1}.

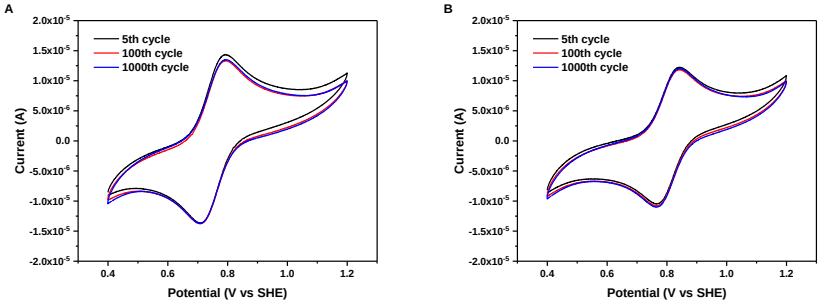

Fig. S3. CV curves of the 5th, 100th, and 1000th cycle at a scan rate of 100 mV s^{-1}. (**A**) 1 mM **NFTEMPO** in 1 M NaCl solution. (**B**) 1 mM **DFTEMPO** in 1 M NaCl solution.

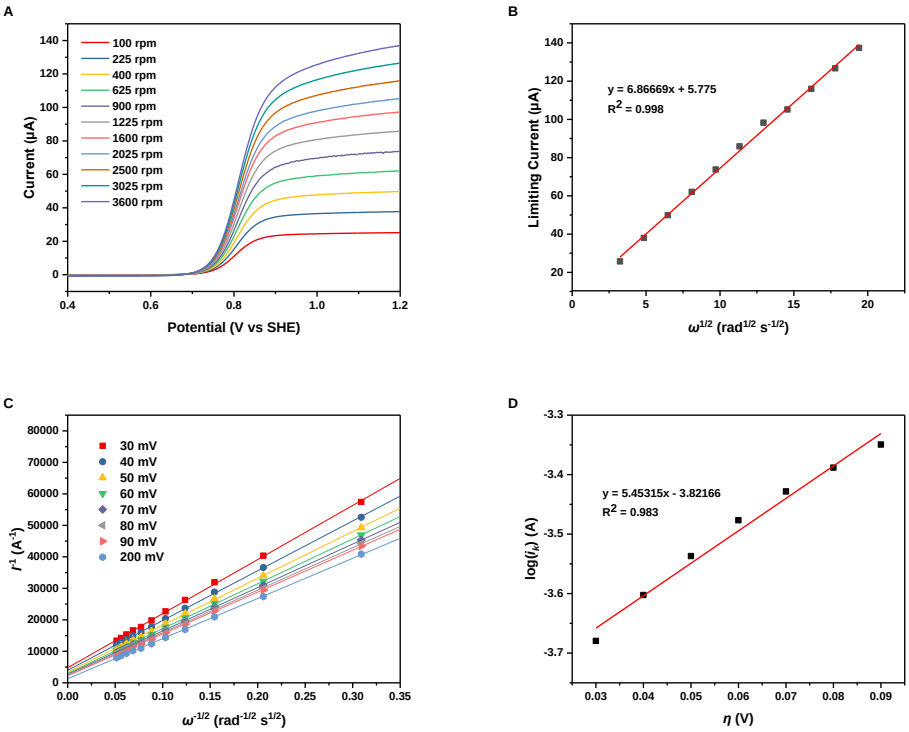

Fig. S4. RDE experiments of **4-HO-TEMPO** (1 mM in 1 M NaCl). (**A**) Current versus potential at varied rotation rates, (**B**) Levich plot of limiting current versus square root of rotation rate ($\omega^{1/2}$), (**C**) Koutecký-Levich plot of reciprocal current versus inverse square root of rotation rate ($\omega^{-1/2}$) at different overpotentials; (**D**) Tafel plot of the logarithm of kinetically limited current versus overpotential. According to the procedure described above, the following constants are obtained: diffusion coefficient $D = 4.43 \times 10^{-6}$ cm² s^{-1}, reaction constant $k_0 = 7.98 \times 10^{-3}$ cm s^{-1} and transfer coefficient $\alpha = 0.32$.

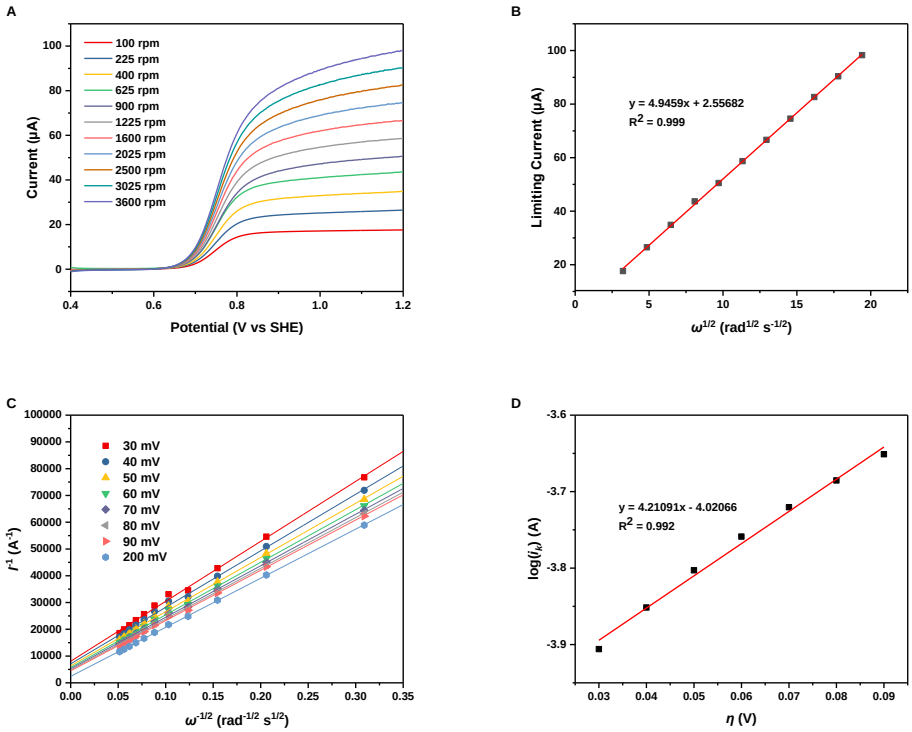

Fig. S5. RDE experiments of **NFTEMPO** (1 mM in 1 M NaCl). (**A**) Current versus potential at varied rotation rates, (**B**) Levich plot of limiting current versus square root of rotation rate ($\omega^{1/2}$), (**C**) Koutecký-Levich plot of reciprocal current versus inverse square root of rotation rate ($\omega^{-1/2}$) at different overpotentials; (**D**) Tafel plot of the logarithm of kinetically limited current versus overpotential. According to the procedure described above, the following constants are obtained: diffusion coefficient $D = 2.71 \times 10^{-6}$ cm² s^{-1}, reaction constant $k_0 = 5.04 \times 10^{-3}$ cm s^{-1} and transfer coefficient $\alpha = 0.25$.

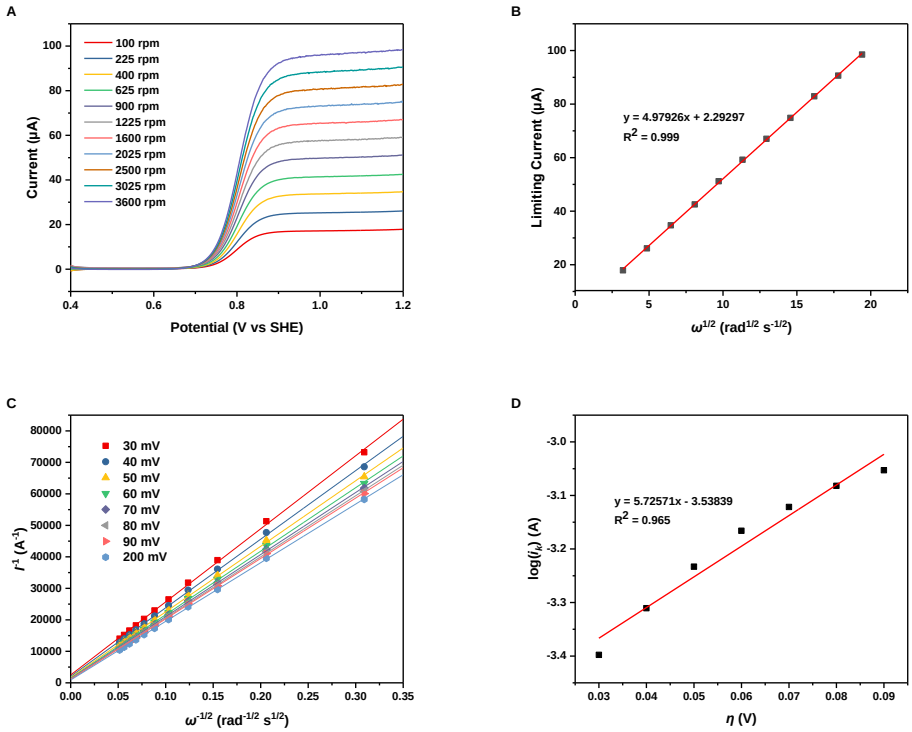

Fig. S6. RDE experiments of **DFTEMPO** (1 mM in 1 M NaCl). (**A**) Current versus potential at varied rotation rates, (**B**) Levich plot of limiting current versus square root of rotation rate ($\omega^{1/2}$), (**C**) Koutecký-Levich plot of reciprocal current versus inverse square root of rotation rate ($\omega^{-1/2}$) at different overpotentials; (**D**) Tafel plot of the logarithm of kinetically limited current versus overpotential. According to the procedure described above, the following constants are obtained: diffusion coefficient $D = 2.74 \times 10^{-6}$ cm² s^{-1}, reaction constant $k_0 = 1.53 \times 10^{-2}$ cm s^{-1} and transfer coefficient $\alpha = 0.34$.

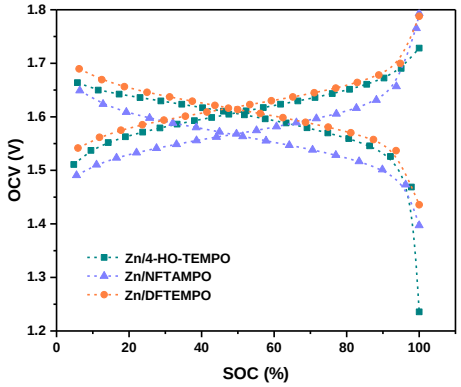

Fig. S7. Open-circuit voltage (OCV) of Zn/**4-HO-TEMPO**, Zn/**NFTEMPO**, and Zn/**DFTEMPO** cells at various states of charge (SOC).

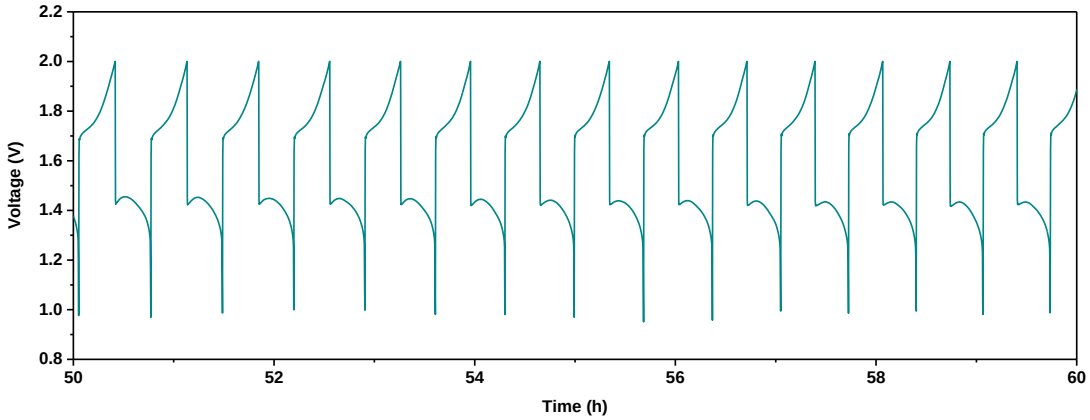

Fig. S8. Representative cell voltage versus time curve during galvanostatic cycling with a current density of 20 mA cm^{-2} for 0.2 M Zn/**4-HO-TEMPO** cell.

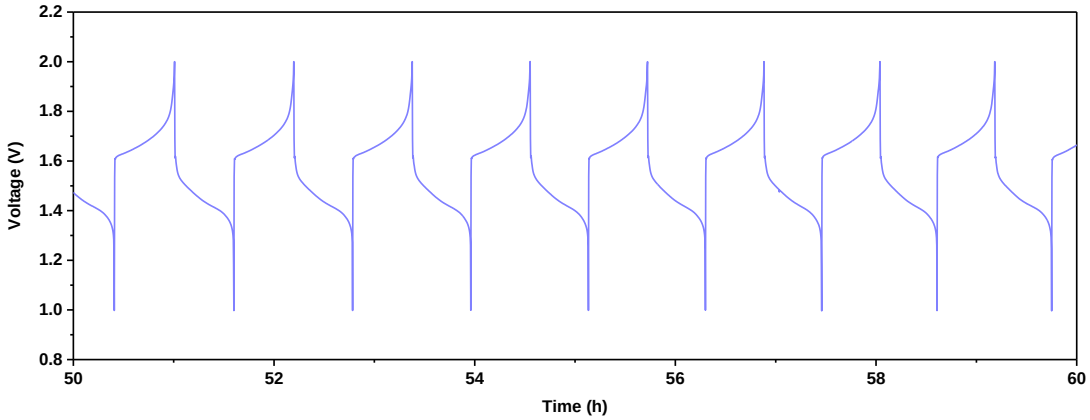

Fig. S9. Representative cell voltage versus time curve during galvanostatic cycling with a current density of 20 mA cm^{-2} for 0.2 M Zn/**NFTEMPO** cell.

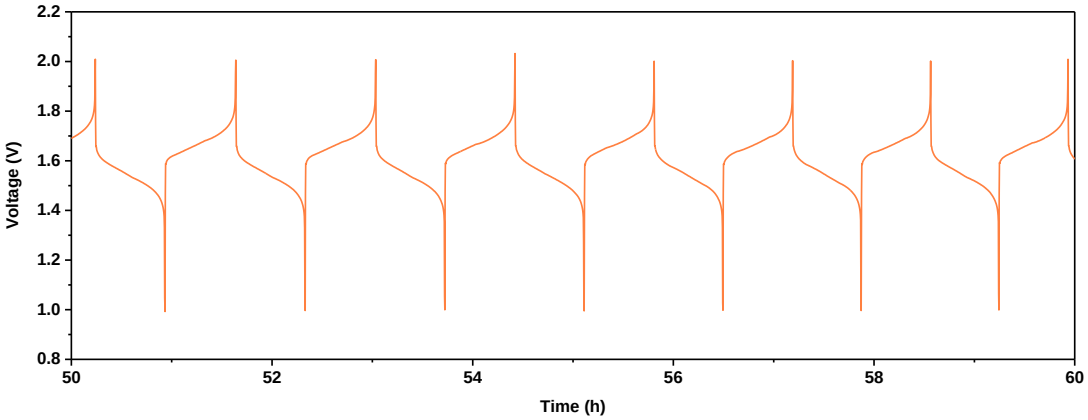

Fig. S10. Representative cell voltage versus time curve during galvanostatic cycling with a current density of 20 mA cm^{-2} for 0.2 M Zn/**DFTEMPO** cell.

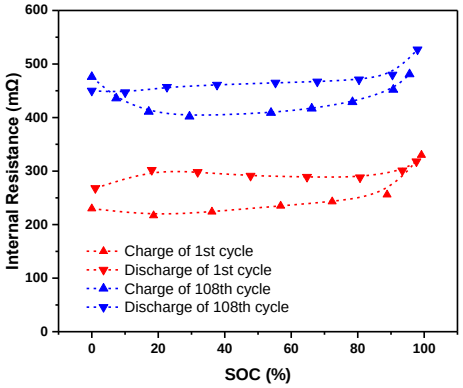

Fig. S11. Internal resistance of the Zn/**DFTEMPO** cell during cycle test.

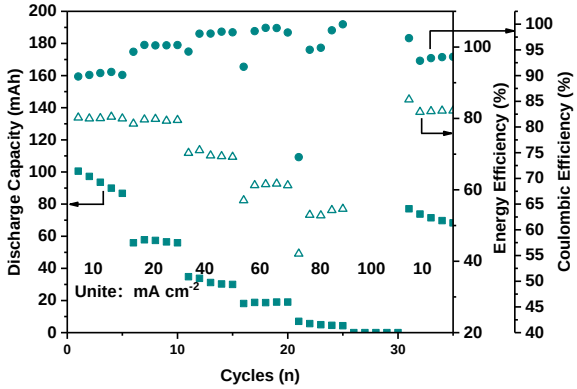

Fig. S12. Rate capability of 0.2M Zn/**4-HO-TEMPO** cell.

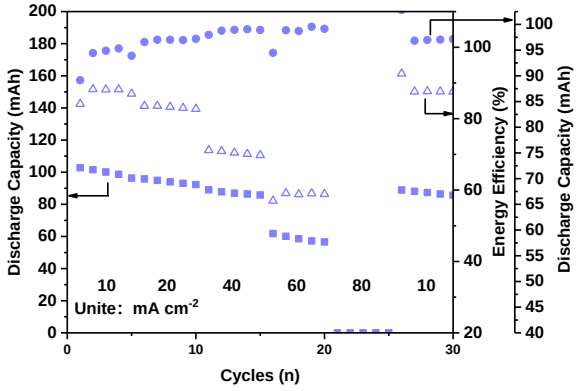

Fig. S13. Rate capability of 0.2M Zn/**NFTEMPO** cell.

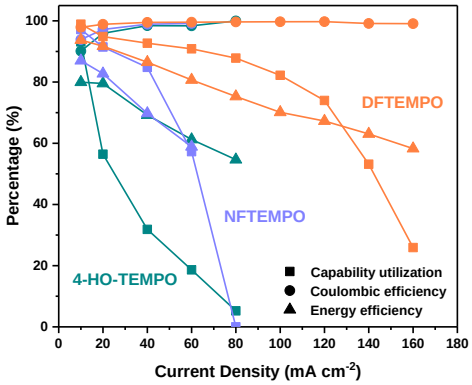

Fig. S14. Capability utilization, Coulombic efficiency (CE) and energy efficiency (EE) of full cells that galvanostatically cycled at varied current densities with 0.2M active concentration.

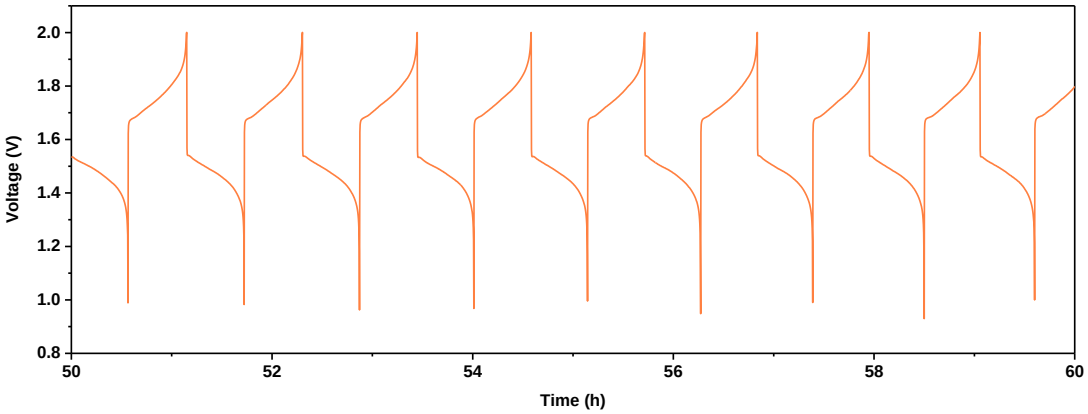

Fig. S15. Representative cell voltage versus time curve during galvanostatic cycling with a current density of 40 mA cm^{-2} for 0.9 M Zn/**DFTEMPO** cell.

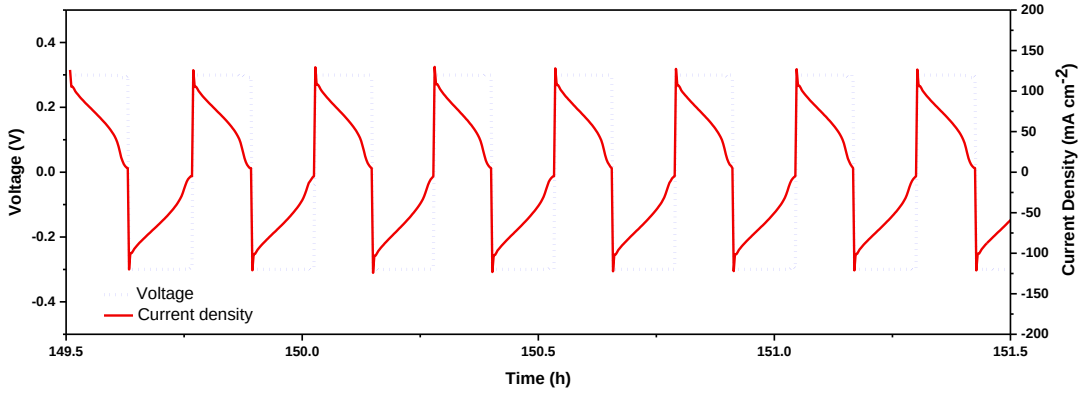

Fig. S16. Representative voltage and current density during potentiostatic cycling (between ±300 mV with a current cutoff of 5 mA cm^{-2}) for 0.1 M **DFTEMPO** symmetric cell.

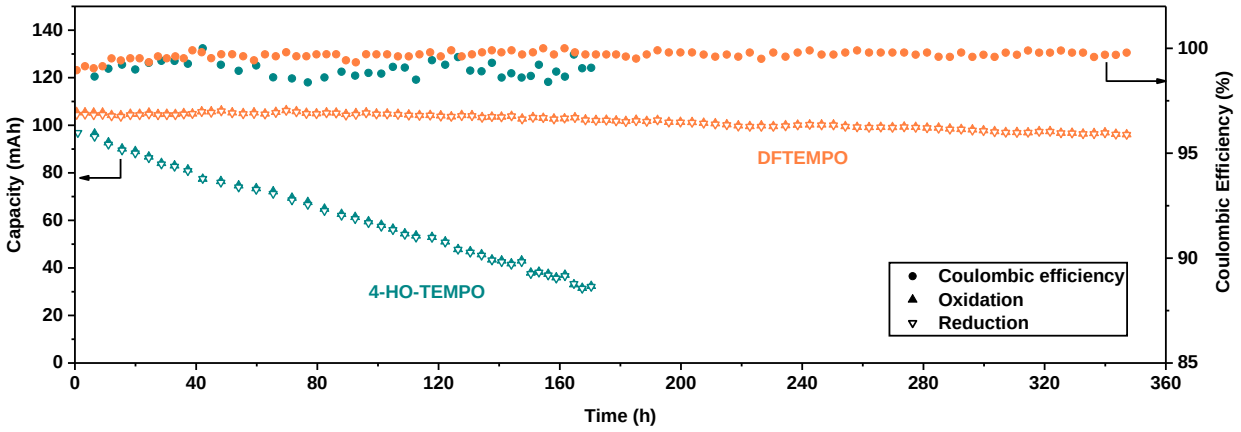

Fig. S17. Potentiostatic cycles of unbalanced compositionally symmetric cells with 0.2 M catholyte material in 2.0 M NH_4Cl. To improve the clarity, one point was taken every five data intervals for plotting. The reduction capacity of DFTEMPO symmetric cell decayed from 104.4 mAh to 96.1 mAh after 500 cycles (~350 h). The reduction capacity of 4-HO-TEMPO symmetric cell decayed from 96.8 mAh to 32.1 mAh after 200 cycles (~170 h).

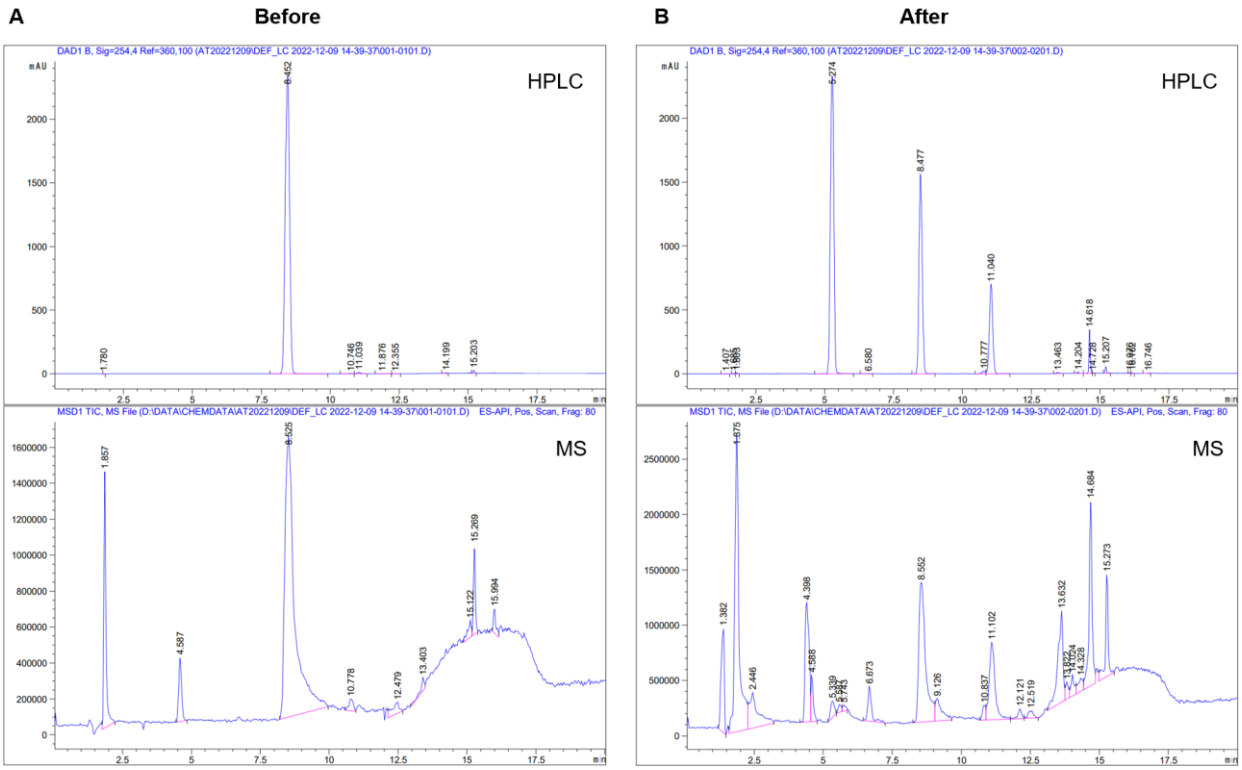

Fig. S18. LC-MS spectra of the **4-HO-TEMPO** catholyte before (**A**) and after (**B**) cycling.

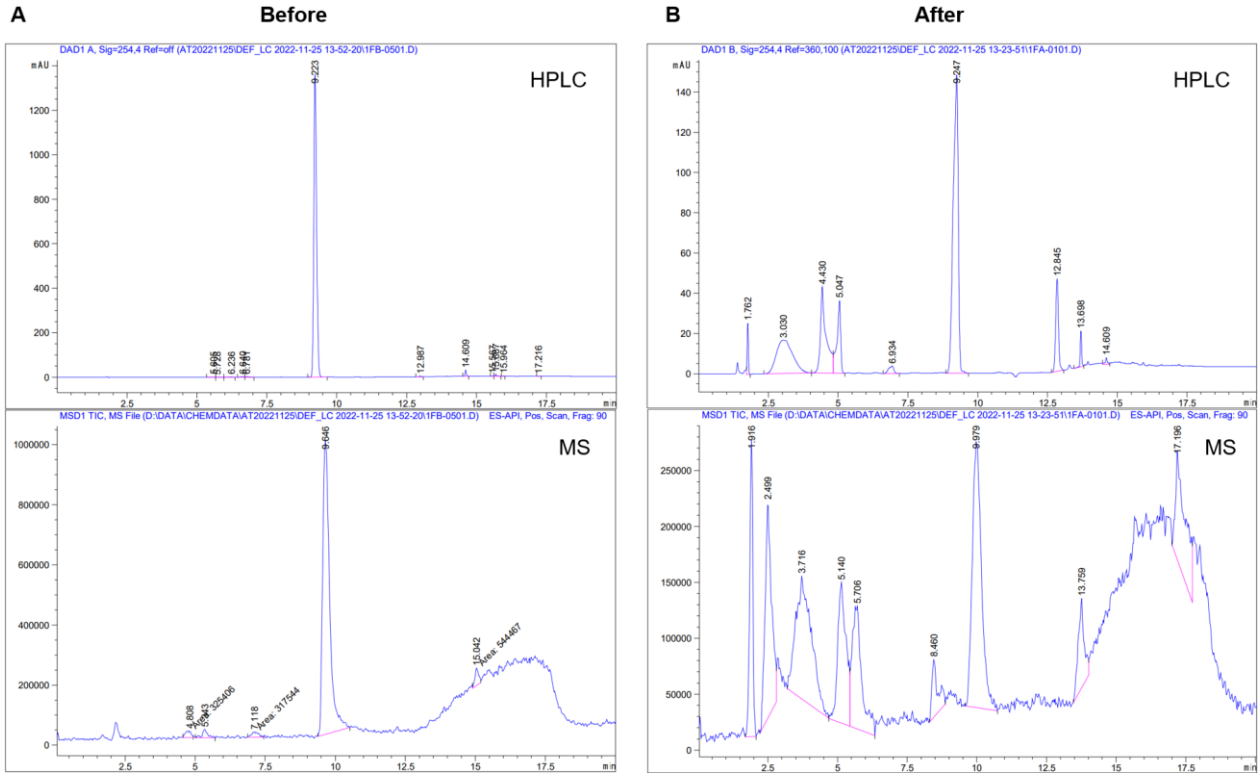

Fig. S19. LC-MS spectra of the **NFTEMPO** catholyte before (**A**) and after (**B**) cycling.

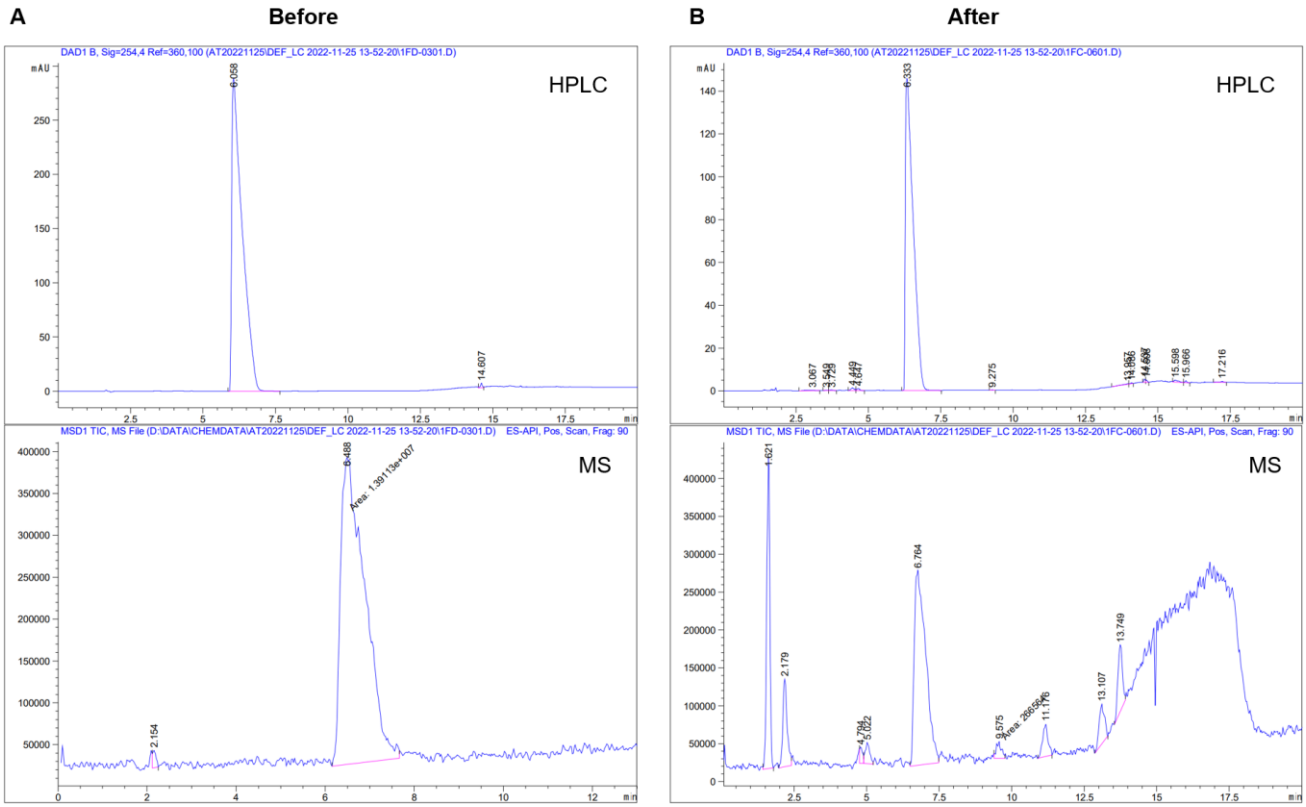

Fig. S20. LC-MS spectra of the **DFTEMPO** catholyte before (**A**) and after (**B**) cycling.

Table S1. Comparison of electrolyte compositions and cell performances of TEMPO-based aqueous redox flow batteries.

Catholyte	Anolyte	Redox Potential (V vs Ag/AgCl)		Cell Voltage (V)	Cycle Time (h)	Capacity Decay Rate (%/h)	Peak Power Density (mW cm^{-2})	Ref.
		Catholyte	Anolyte					
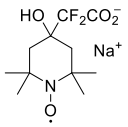	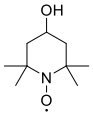	0.606	-1.031	1.64	134	0.195	244.9	This Work
		0.61	-0.98	1.59	N.A.	1.1 (per cycle)	N.A.	1
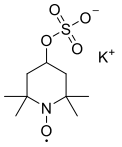	Zn^{2+}	0.61	-1.08	1.69	55.6	N.A.	N.A.	2
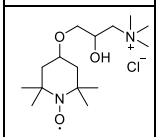		N.A.	N.A.	1.55	~70	0.092	N.A.	3
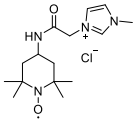		0.63	N.A.	1.71	280	0.0019	186.7	4
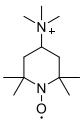	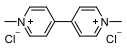	0.79	-0.63	1.4	N.A.	0.046	N.A.	5
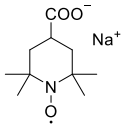	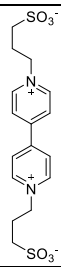	0.60	-0.59	1.19	N.A.	0.06 (per cycle)	N.A.	6
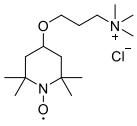	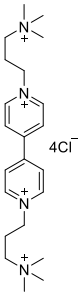	0.81 (vs SHE)	-0.38 (vs SHE)	1.12	220	0.026	99.03	7

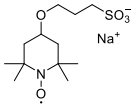	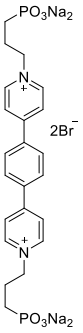	0.805 (vs SHE)	-0.801 (vs SHE)	1.61	264	N.A.	405	8
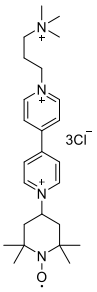	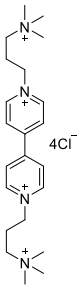	0.967 (vs SHE)	-0.332 (vs SHE)	1.30	N.A.	0.02 (per cycle)	N.A.	9

Table S2. Comparison of symmetric-cell performances of TEMPO-based aqueous redox flow batteries.

Catholyte	Concentration (M)	No. of Cycles	Cycle Time (h)	Capacity Decay Rate (%/h)	Ref.
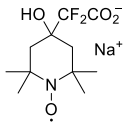	0.1	1000	250	0.022	This Work
	0.2	500	350	0.023	
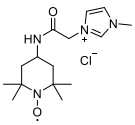	0.1	200	57	0.002	4
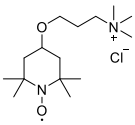	0.1	1,850	600	0.023	7
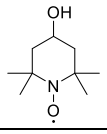	0.2	200	N.A.	0.282 (per cycle)	10
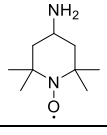	0.2	200	N.A.	0.385 (per cycle)	10

4. DFT Data

4.1 Optimized Structures

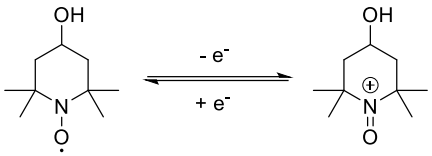

4-HO-TEMPO 4-HO-TEMPO^{+}

Optimized Structure of **4-HO-TEMPO**:

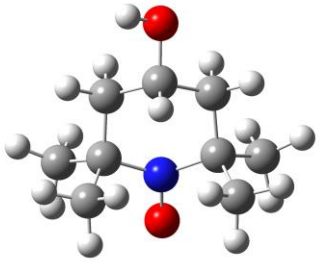

Standard orientation:

Center Number	Atomic Number	Atomic Type	Coordinates (Angstroms) X	Y	Z
1	6	0	1.754482	-0.440251	0.192832
2	6	0	0.791243	-1.482035	-0.354845
3	6	0	-0.685315	-1.205317	-0.005711
4	1	0	0.905270	-1.508686	-1.445821
5	1	0	1.046211	-2.475958	0.027260
6	1	0	1.726922	-0.429036	1.288635
7	7	0	-1.004489	0.246963	-0.258901
8	8	0	-2.259453	0.556429	-0.288508
9	6	0	-0.044352	1.383163	-0.010934
10	8	0	3.081244	-0.826452	-0.223690
11	1	0	3.709854	-0.190845	0.150648
12	6	0	1.385734	0.930744	-0.367013
13	1	0	1.491448	0.889202	-1.458222
14	1	0	2.081237	1.692788	0.002519
15	6	0	-0.151477	1.831426	1.462593
16	1	0	0.449294	2.735728	1.602297
17	1	0	-1.190134	2.066884	1.712678
18	1	0	0.211413	1.072861	2.159421
19	6	0	-0.441284	2.554427	-0.922627
20	1	0	-1.412994	2.968664	-0.644930
21	1	0	0.308527	3.345113	-0.821011

22	1	0	-0.474059	2.247944	-1.972541
23	6	0	-1.578241	-2.058306	-0.920206
24	1	0	-1.275980	-3.105657	-0.823393
25	1	0	-2.632000	-1.981208	-0.643499
26	1	0	-1.466067	-1.766493	-1.968889
27	6	0	-0.995265	-1.546163	1.468131
28	1	0	-2.016995	-1.247064	1.720076
29	1	0	-0.910481	-2.628647	1.607338
30	1	0	-0.307525	-1.060282	2.164007

Optimized Structure of **4-HO-TEMPO**$^{+}$:

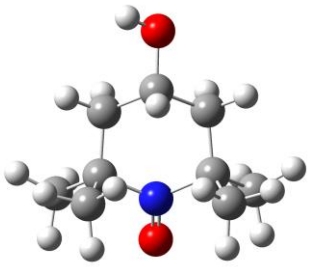

Standard orientation:

Center Number	Atomic Number	Atomic Type	Coordinates (Angstroms) X	Y	Z
1	6	0	1.529858	-0.977022	0.160250
2	6	0	0.270722	-1.657381	-0.360365
3	6	0	-1.041901	-0.949604	0.024568
4	1	0	0.333455	-1.716973	-1.452825
5	1	0	0.197392	-2.677437	0.027624
6	1	0	1.539486	-0.971307	1.255665
7	7	0	-0.885867	0.562422	-0.203004
8	8	0	-1.855618	1.178722	-0.531565
9	6	0	0.417418	1.344744	0.017691
10	8	0	2.641792	-1.754561	-0.308710
11	1	0	3.451928	-1.381870	0.071106
12	6	0	1.605066	0.449349	-0.384244
13	1	0	1.663250	0.402913	-1.477463
14	1	0	2.507086	0.952124	-0.021046
15	6	0	0.433593	1.732616	1.518999
16	1	0	1.256831	2.443243	1.633738
17	1	0	-0.498821	2.227979	1.800540
18	1	0	0.616037	0.885548	2.178961

19	6	0	0.348770	2.605770	-0.844403
20	1	0	-0.419820	3.297260	-0.494087
21	1	0	1.320440	3.099488	-0.764101
22	1	0	0.167723	2.360538	-1.894514
23	6	0	-2.203220	-1.429006	-0.848699
24	1	0	-2.240993	-2.517617	-0.759850
25	1	0	-3.159427	-1.021479	-0.516430
26	1	0	-2.040905	-1.170794	-1.898799
27	6	0	-1.404390	-1.116930	1.522190
28	1	0	-2.266717	-0.497709	1.780024
29	1	0	-1.675900	-2.168612	1.648129
30	1	0	-0.574858	-0.890751	2.190625

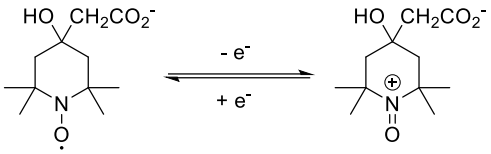

NFTEMPO NFTEMPO$^+$

Optimized Structure of **NFTEMPO**:

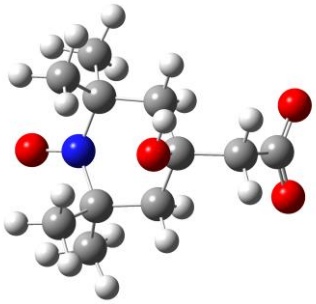

Standard orientation:

Center Number	Atomic Number	Atomic Type	Coordinates (Angstroms) X	Y	Z
1	6	0	0.869693	-0.048451	0.829897
2	6	0	0.299752	-1.283712	0.131296
3	6	0	-1.224793	-1.312812	-0.121205
4	1	0	0.803143	-1.363078	-0.836387
5	1	0	0.563822	-2.181952	0.699512
6	7	0	-1.695611	0.031496	-0.603521
7	8	0	-2.885419	0.068616	-1.111821
8	6	0	-1.126946	1.347703	-0.149753
9	6	0	0.391726	1.210308	0.094688

10	1	0	0.892163	1.227611	-0.878718
11	1	0	0.726174	2.102658	0.636531
12	6	0	-1.893798	1.832855	1.099928
13	1	0	-1.539961	2.834286	1.366388
14	1	0	-2.964389	1.895931	0.882828
15	1	0	-1.744370	1.179189	1.959304
16	6	0	-1.334846	2.371561	-1.280216
17	1	0	-2.394106	2.579847	-1.446054
18	1	0	-0.843373	3.307590	-0.997173
19	1	0	-0.891542	2.023867	-2.218406
20	6	0	-1.496779	-2.340243	-1.235131
21	1	0	-1.066748	-3.301345	-0.936235
22	1	0	-2.566709	-2.483428	-1.401270
23	1	0	-1.030834	-2.036858	-2.177713
24	6	0	-2.037448	-1.713777	1.129193
25	1	0	-3.106510	-1.715327	0.895963
26	1	0	-1.751745	-2.726997	1.430488
27	1	0	-1.860253	-1.045468	1.971654
28	8	0	0.401802	-0.070746	2.200820
29	1	0	0.714636	0.738324	2.634300
30	6	0	2.422944	-0.100845	0.905877
31	6	0	3.193901	-0.048142	-0.422322
32	8	0	3.601601	1.087262	-0.827504
33	8	0	3.397416	-1.143131	-1.037344
34	1	0	2.686644	-1.024934	1.429943
35	1	0	2.739596	0.746941	1.522971

Optimized Structure of **NFTEMPO**$^{+}$:

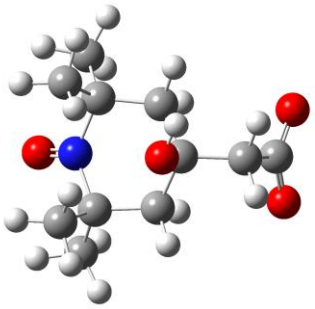

Standard orientation:

Center Number	Atomic Number	Atomic Type	Coordinates (Angstroms) X	Y	Z

1	6	0	0.867195	-0.042513	0.847086
2	6	0	0.303988	-1.283662	0.151032
3	6	0	-1.221315	-1.332583	-0.096269
4	1	0	0.799646	-1.376902	-0.818291
5	1	0	0.552385	-2.178704	0.728782
6	7	0	-1.693212	0.029528	-0.605664
7	8	0	-2.579285	0.050508	-1.409738
8	6	0	-1.132436	1.367083	-0.124328
9	6	0	0.386330	1.221509	0.118635
10	1	0	0.881331	1.262522	-0.855616
11	1	0	0.697022	2.112286	0.674569
12	6	0	-1.942078	1.744642	1.144867
13	1	0	-1.658305	2.773415	1.384376
14	1	0	-3.013864	1.717596	0.932258
15	1	0	-1.710591	1.113321	1.998595
16	6	0	-1.401875	2.402291	-1.220269
17	1	0	-2.467938	2.605811	-1.336723
18	1	0	-0.905217	3.326476	-0.914039
19	1	0	-0.984990	2.086228	-2.180261
20	6	0	-1.552936	-2.368879	-1.174048
21	1	0	-1.112492	-3.316259	-0.853013
22	1	0	-2.629079	-2.510245	-1.288232
23	1	0	-1.118273	-2.093209	-2.138746
24	6	0	-2.057390	-1.630531	1.175973
25	1	0	-3.124889	-1.585395	0.946749
26	1	0	-1.803643	-2.653981	1.466040
27	1	0	-1.819989	-0.968821	2.004191
28	8	0	0.404818	-0.070230	2.213547
29	1	0	0.749158	0.716888	2.664235
30	6	0	2.420176	-0.090565	0.901753
31	6	0	3.170573	-0.046297	-0.440083
32	8	0	3.572051	1.086383	-0.855815
33	8	0	3.358687	-1.145659	-1.050393
34	1	0	2.689826	-1.010796	1.428662
35	1	0	2.740833	0.762096	1.509212

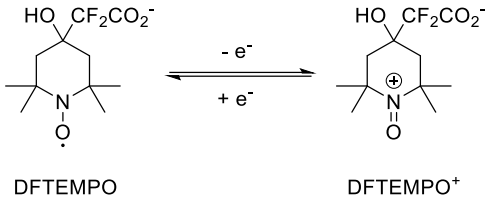

Optimized Structure of **DFTEMPO**:

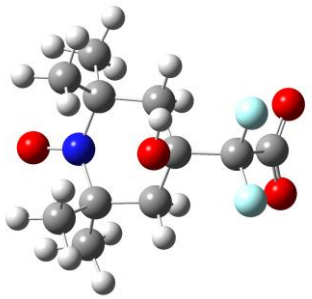

Standard orientation:

Center Number	Atomic Number	Atomic Type	Coordinates (Angstroms) X	Y	Z
1	6	0	0.616793	-0.048649	0.581574
2	6	0	-0.016685	-1.275134	-0.080378
3	6	0	-1.561318	-1.307539	-0.126856
4	1	0	0.354477	-1.321889	-1.107404
5	1	0	0.321896	-2.183519	0.425228
6	7	0	-2.094356	0.041146	-0.523407
7	8	0	-3.336273	0.079252	-0.881266
8	6	0	-1.490262	1.348056	-0.089023
9	6	0	0.049130	1.230212	-0.051437
10	1	0	0.415331	1.282087	-1.080676
11	1	0	0.438585	2.110903	0.469579
12	6	0	-2.090566	1.770064	1.269033
13	1	0	-1.724050	2.770202	1.521869
14	1	0	-3.181430	1.812711	1.197525
15	1	0	-1.814218	1.092114	2.076295
16	6	0	-1.853476	2.413666	-1.138356
17	1	0	-2.926380	2.616762	-1.147184
18	1	0	-1.333264	3.343100	-0.886867
19	1	0	-1.542128	2.108638	-2.142075
20	6	0	-1.970435	-2.323078	-1.208258
21	1	0	-1.514863	-3.288991	-0.968974
22	1	0	-3.053577	-2.456853	-1.243074
23	1	0	-1.619024	-2.016829	-2.198312

24	6	0	-2.199883	-1.734348	1.212146
25	1	0	-3.289529	-1.748239	1.115079
26	1	0	-1.865033	-2.747173	1.458242
27	1	0	-1.926184	-1.075643	2.035537
28	8	0	0.374119	-0.126228	1.991050
29	1	0	0.621706	0.717130	2.401162
30	6	0	2.169584	-0.080770	0.400086
31	6	0	2.756262	0.060820	-1.045013
32	8	0	3.081382	1.221926	-1.403179
33	8	0	2.839174	-1.005950	-1.707435
34	9	0	2.652320	-1.255570	0.958023
35	9	0	2.700580	0.925089	1.197915

Optimized Structure of **DFTEMPO**$^{+}$:

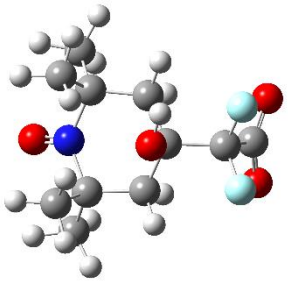

Standard orientation:

Center Number	Atomic Number	Atomic Type	Coordinates (Angstroms) X	Y	Z
1	6	0	0.619495	-0.047332	0.597216
2	6	0	-0.013036	-1.279119	-0.057802
3	6	0	-1.555787	-1.328305	-0.099344
4	1	0	0.351081	-1.344163	-1.085489
5	1	0	0.310968	-2.184300	0.461508
6	7	0	-2.103390	0.041024	-0.494364
7	8	0	-3.111946	0.076680	-1.135959
8	6	0	-1.484239	1.370816	-0.061442
9	6	0	0.052788	1.236306	-0.031156
10	1	0	0.409555	1.305458	-1.061798
11	1	0	0.428920	2.115546	0.500086
12	6	0	-2.113395	1.713312	1.315219
13	1	0	-1.791143	2.733391	1.542516
14	1	0	-3.203779	1.695425	1.249396

15	1	0	-1.772407	1.055968	2.111015
16	6	0	-1.902694	2.428920	-1.087020
17	1	0	-2.975565	2.625024	-1.051575
18	1	0	-1.374658	3.350489	-0.829468
19	1	0	-1.617669	2.136233	-2.101157
20	6	0	-2.018257	-2.337591	-1.154533
21	1	0	-1.535965	-3.289345	-0.917337
22	1	0	-3.099177	-2.483870	-1.131361
23	1	0	-1.710748	-2.033151	-2.158557
24	6	0	-2.221073	-1.669030	1.261012
25	1	0	-3.308658	-1.616902	1.169041
26	1	0	-1.934835	-2.701508	1.480527
27	1	0	-1.879828	-1.034361	2.074217
28	8	0	0.384082	-0.126156	2.002418
29	1	0	0.665142	0.702407	2.422314
30	6	0	2.171286	-0.080698	0.390570
31	6	0	2.730184	0.058019	-1.066909
32	8	0	3.065320	1.215354	-1.424917
33	8	0	2.776330	-1.007860	-1.732903
34	9	0	2.654531	-1.255729	0.940773
35	9	0	2.707756	0.925124	1.179527

4.2 Condensed Fukui Functions and Condensed Local Softnesses

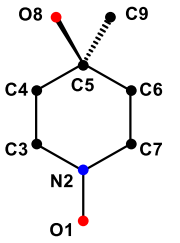

Molecular skeleton of
TEMPO species
(C9 atom only exists in NFTEMPO and DFTEMPO)

Table S3. Hirshfeld charges and condensed Fukui functions of key atoms in **4-HO-TEMPO** and **4-HO-TEMPO$^+$**. Units used below are "e" (elementary charge).

Atom	Hirshfeld charge of 4-HO-TEMPO		Hirshfeld charge of 4-HO-TEMPO$^+$		Condensed Fukui function	
	$q_{(N)}$	$q_{(N-1)}$	$q^+_{(N)}$	$q^+_{(N+1)}$	f^- $q_{(N-1)} - q_{(N)}$	f^+ $q^+_{(N)} - q^+_{(N+1)}$
O1	-0.3160	-0.0159	0.0054	-0.3044	**0.3000**	**0.3098**
N2	0.0858	0.2735	0.2759	0.0827	**0.1877**	**0.1932**
C3	0.0715	0.0932	0.0930	0.0718	**0.0217**	**0.0212**
C4	-0.0558	-0.0465	-0.0448	-0.0569	**0.0093**	**0.0121**
C5	0.0555	0.0588	0.0613	0.0574	**0.0033**	**0.0040**
C6	-0.0547	-0.0456	-0.0443	-0.0562	**0.0090**	**0.0119**
C7	0.0710	0.0927	0.0923	0.0711	**0.0216**	**0.0212**
O8	-0.2721	-0.2617	-0.2585	-0.2696	**0.0104**	**0.0111**

Table S4. Hirshfeld charges and condensed Fukui functions of key atoms in **NFTEMPO** and **NFTEMPO$^+$**. Units used below are "e" (elementary charge).

Atom	Hirshfeld charge of NFTEMPO		Hirshfeld charge of NFTEMPO$^+$		Condensed Fukui function	
	$q_{(N)}$	$q_{(N-1)}$	$q^+_{(N)}$	$q^+_{(N+1)}$	f^- $q_{(N-1)} - q_{(N)}$	f^+ $q^+_{(N)} - q^+_{(N+1)}$
O1	-0.3192	-0.0215	0.0003	-0.3069	**0.2977**	**0.3072**
N2	0.0868	0.2733	0.2747	0.0835	**0.1865**	**0.1913**
C3	0.0691	0.0906	0.0895	0.0689	**0.0215**	**0.0206**
C4	-0.0575	-0.0498	-0.0478	-0.0589	**0.0076**	**0.0111**
C5	0.0939	0.0951	0.0972	0.0956	**0.0012**	**0.0016**
C6	-0.0589	-0.0510	-0.0490	-0.0603	**0.0079**	**0.0114**
C7	0.0691	0.0906	0.0897	0.0689	**0.0216**	**0.0208**
O8	-0.2352	-0.2296	-0.2226	-0.2284	**0.0056**	**0.0058**
C9	-0.0758	-0.0714	-0.0710	-0.0760	**0.0044**	**0.0050**

Table S5. Hirshfeld charges and condensed Fukui functions of key atoms in **DFTEMPO** and **DFTEMPO$^+$**. Units used below are "e" (elementary charge).

Atom	Hirshfeld charge of DFTEMPO		Hirshfeld charge of DFTEMPO$^+$		Condensed Fukui function	
	$q_{(N)}$	$q_{(N-1)}$	$q^+_{(N)}$	$q^+_{(N+1)}$	f^- $q_{(N-1)} - q_{(N)}$	f^+ $q^+_{(N)} - q^+_{(N+1)}$
O1	-0.3130	-0.0146	0.0056	-0.3025	**0.2985**	**0.3081**
N2	0.0860	0.2732	0.2756	0.0836	**0.1873**	**0.1920**
C3	0.0710	0.0926	0.0918	0.0711	**0.0216**	**0.0208**
C4	-0.0571	-0.0491	-0.0478	-0.0585	**0.0080**	**0.0107**
C5	0.0754	0.0764	0.0783	0.0770	**0.0011**	**0.0013**
C6	-0.0600	-0.0518	-0.0507	-0.0617	**0.0083**	**0.0110**
C7	0.0708	0.0925	0.0915	0.0707	**0.0217**	**0.0208**
O8	-0.2288	-0.2228	-0.2175	-0.2237	**0.0061**	**0.0062**
C9	0.1700	0.1730	0.1726	0.1692	**0.0030**	**0.0034**

5. Copies of ^{1}H NMR, ^{19}F NMR and ^{13}C NMR Spectra

Benzyl 2,2,6,6-tetramethyl-4-oxopiperidine-1-carboxylate (2).

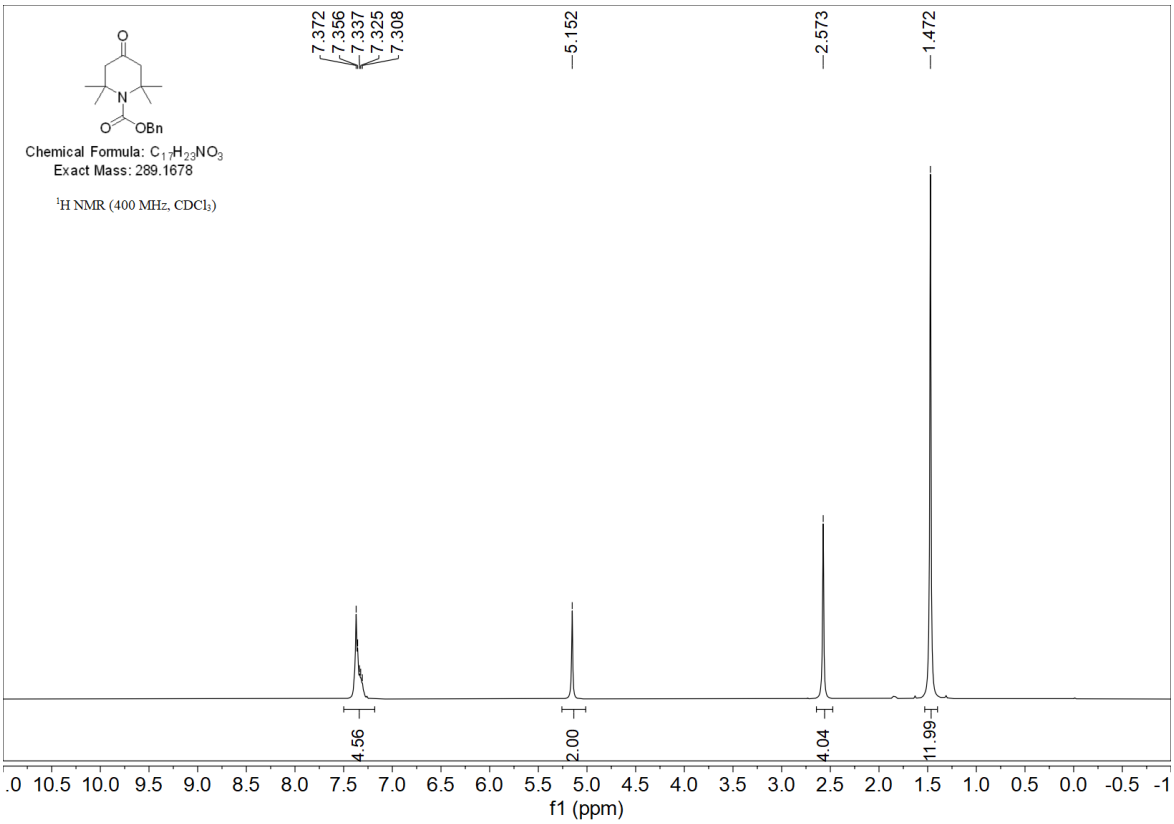

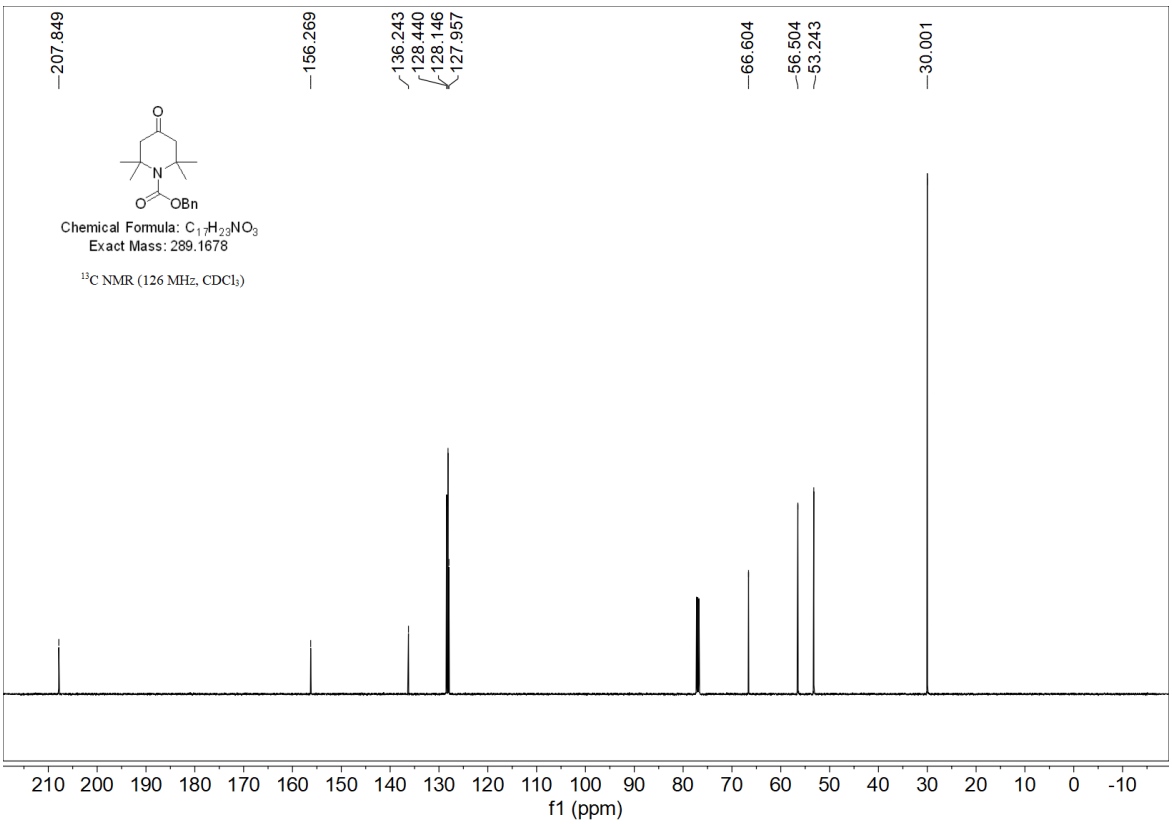

Benzyl 4-(2-ethoxy-1,1-difluoro-2-oxoethyl)-4-hydroxy-2,2,6,6-tetramethylpiperidine-1-carboxylate (3a).

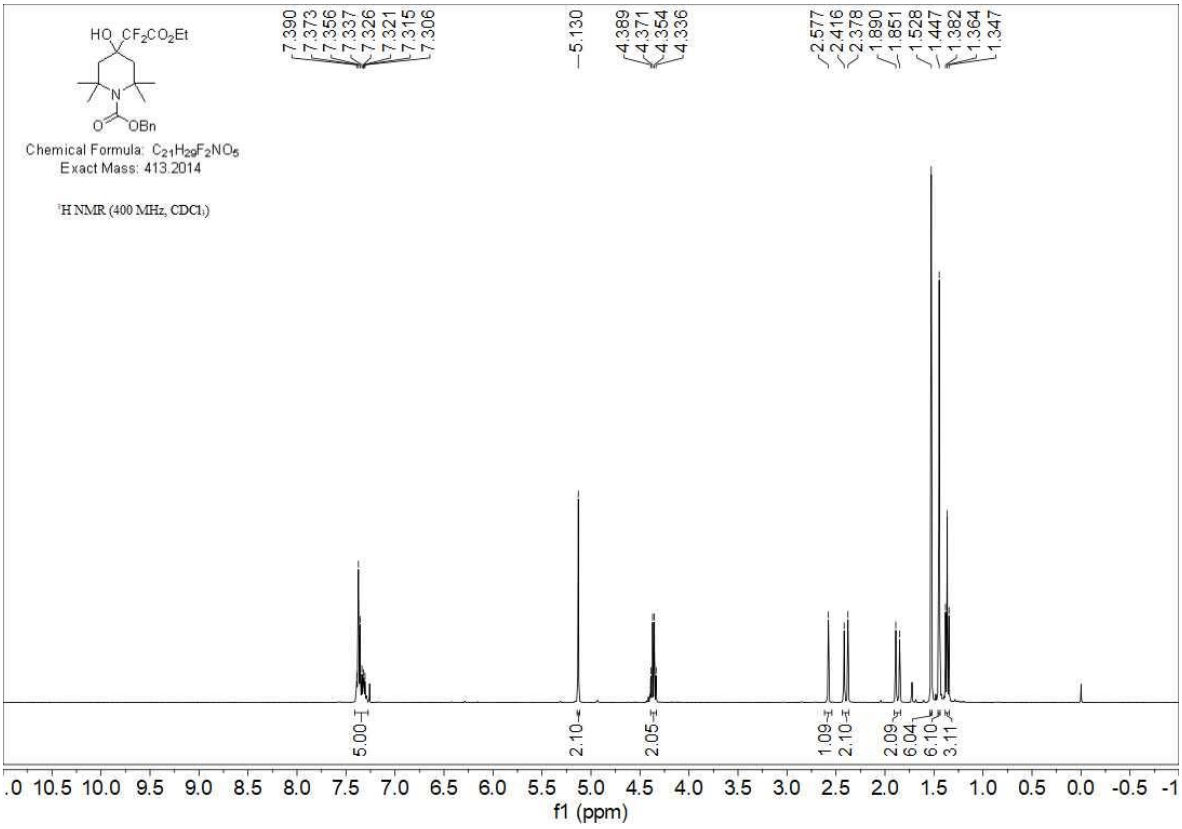

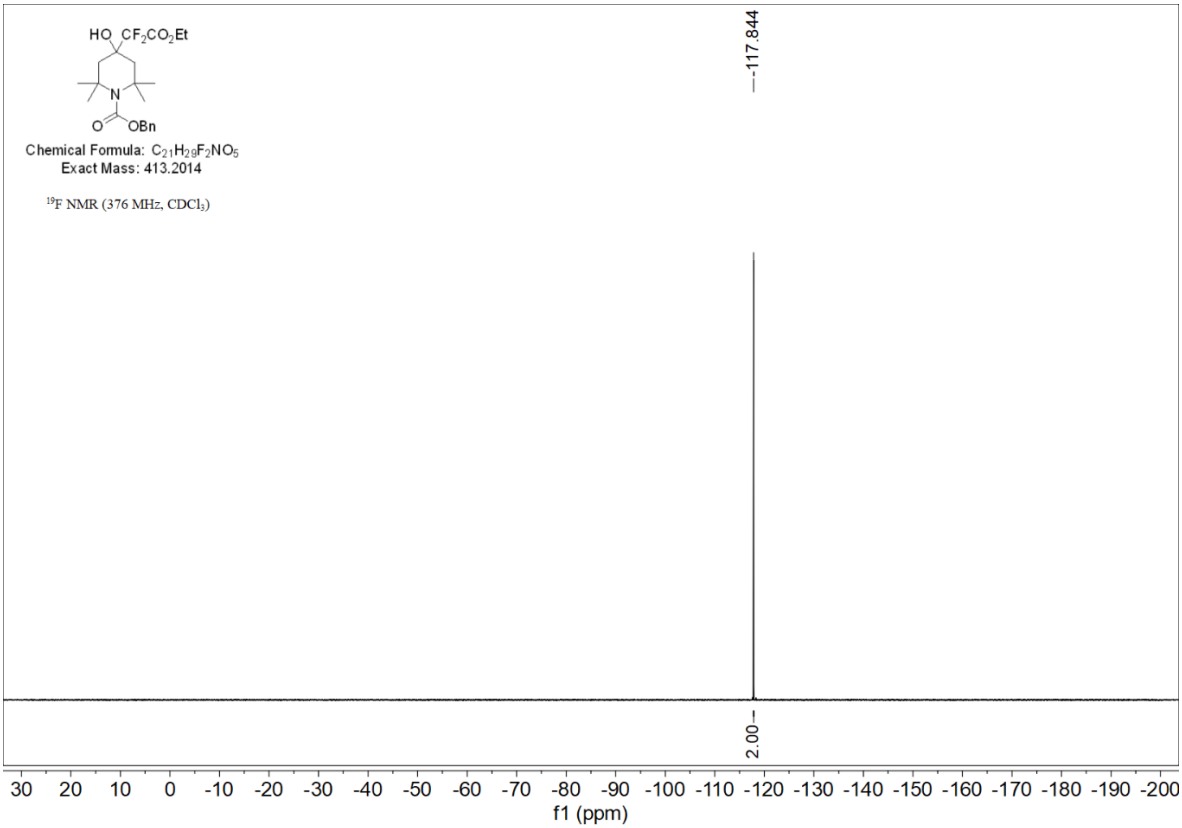

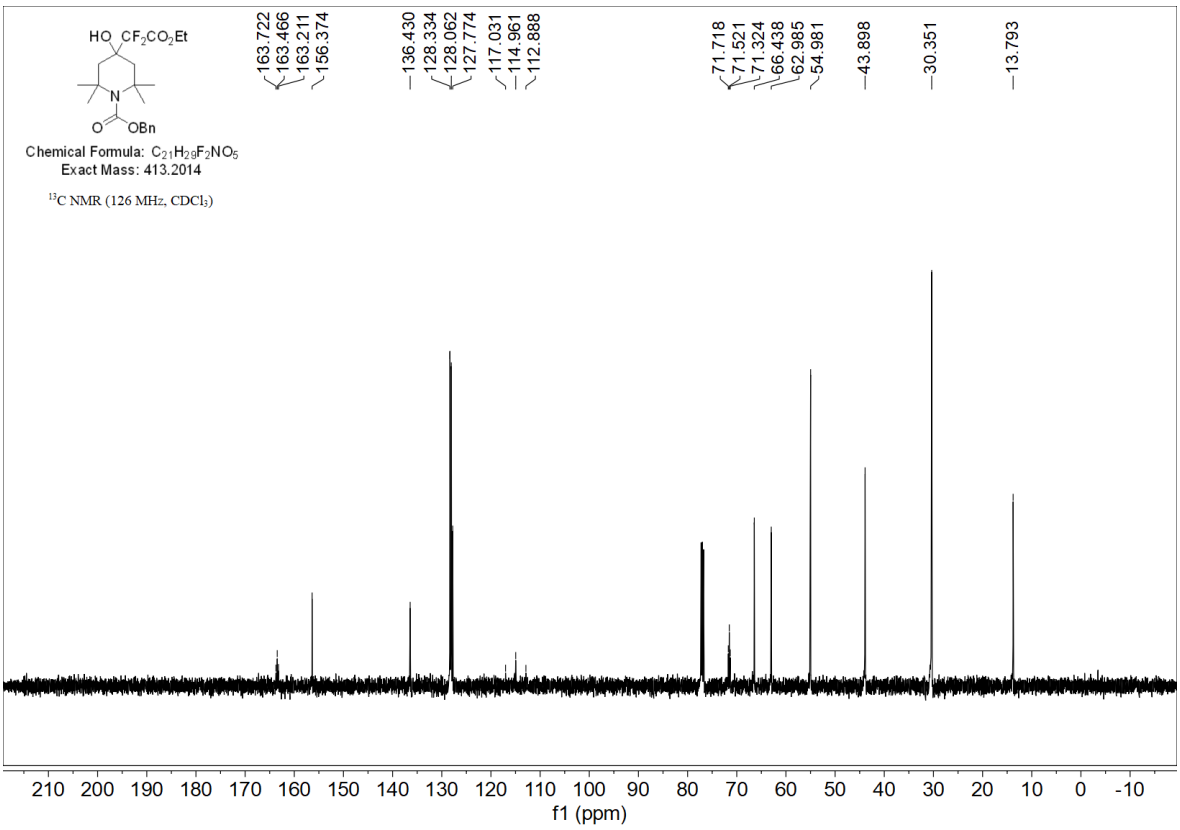

Benzyl 4-(2-ethoxy-2-oxoethyl)-4-hydroxy-2,2,6,6-tetramethylpiperidine-1-carboxylate (3b).

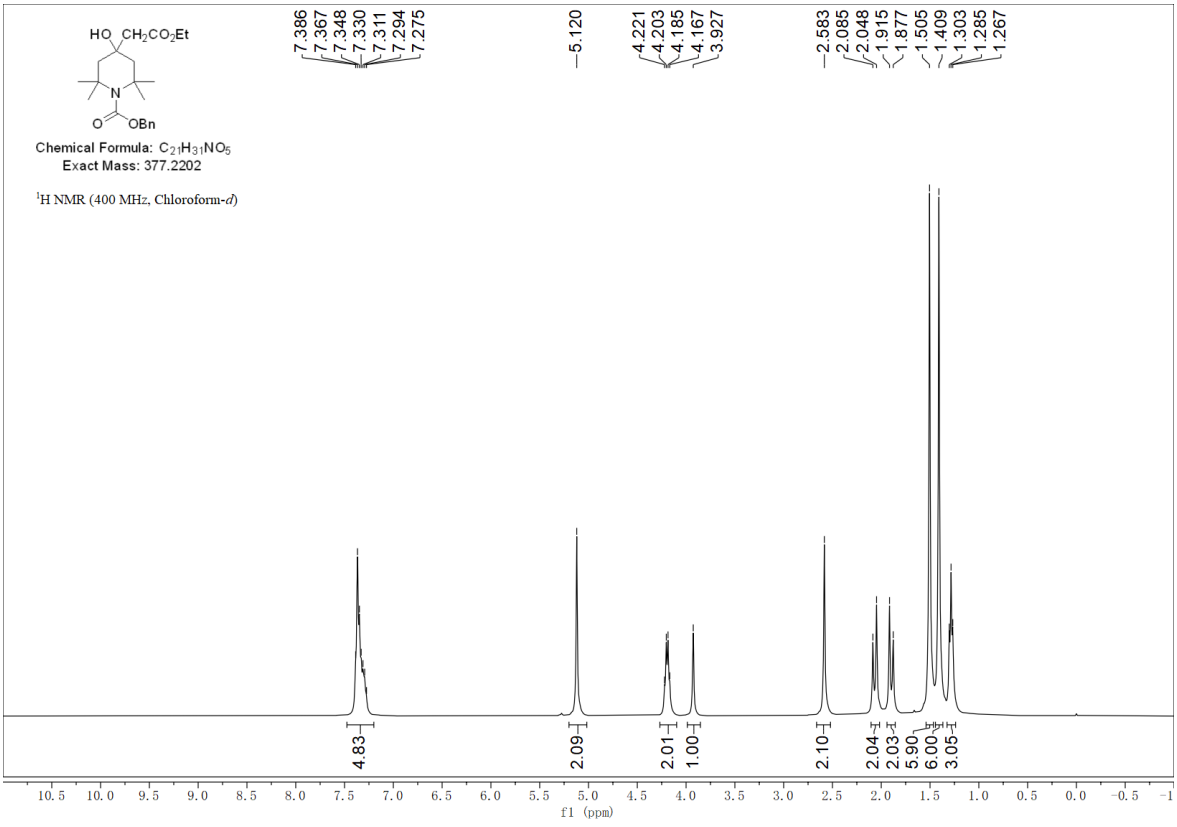

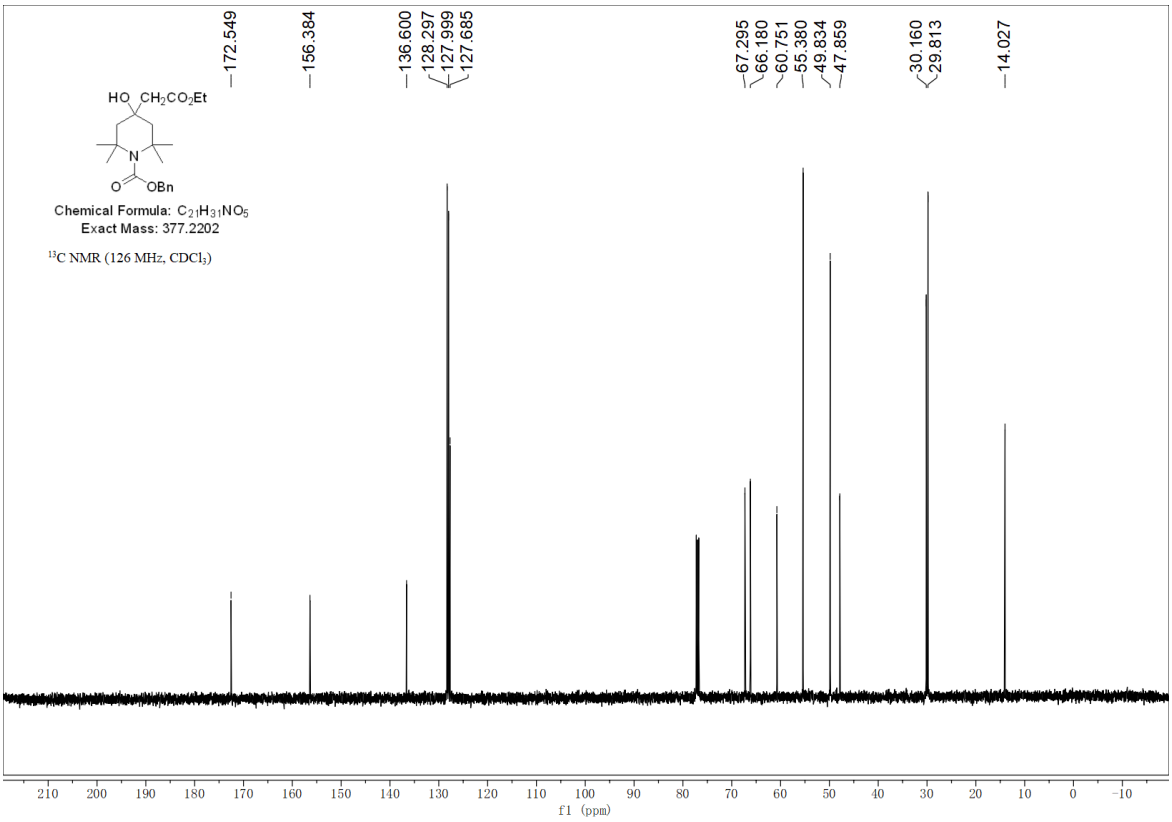

Ethyl 2-(4-hydroxy-2,2,6,6-tetramethylpiperidin-4-yl)-2,2-difluoroacetate (F3).

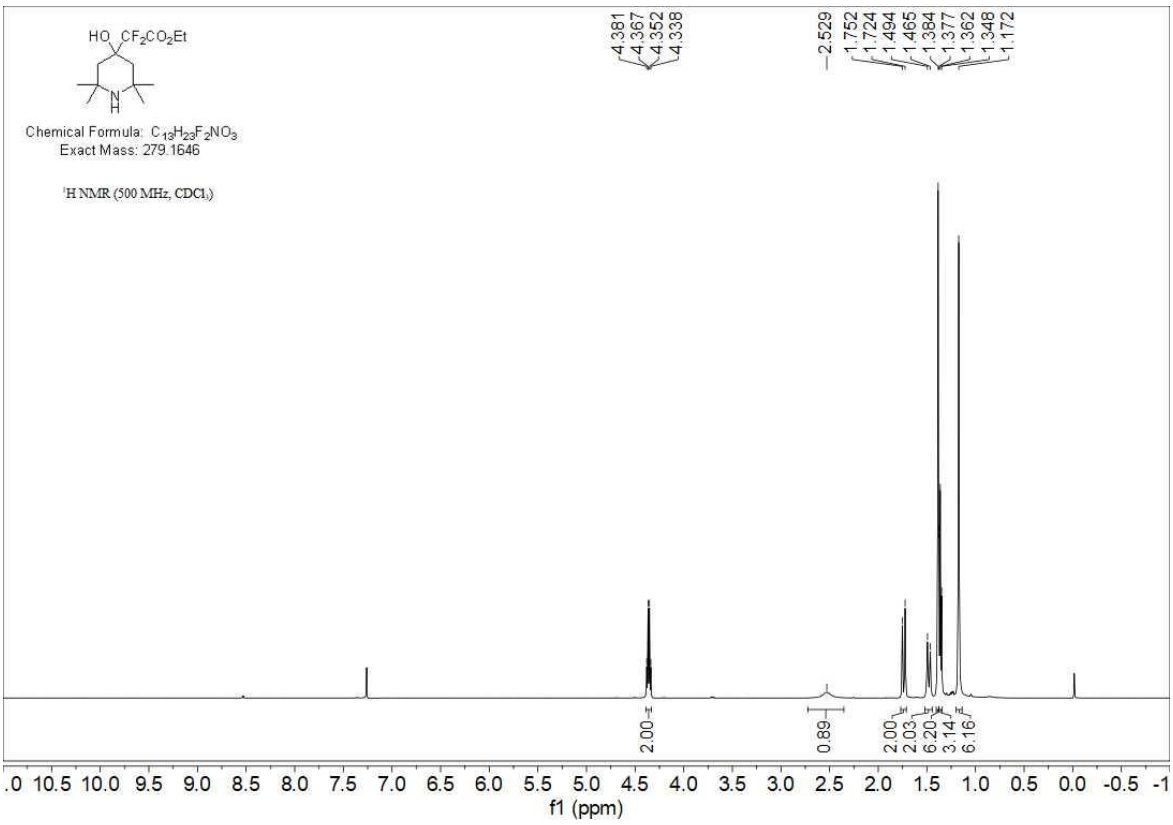

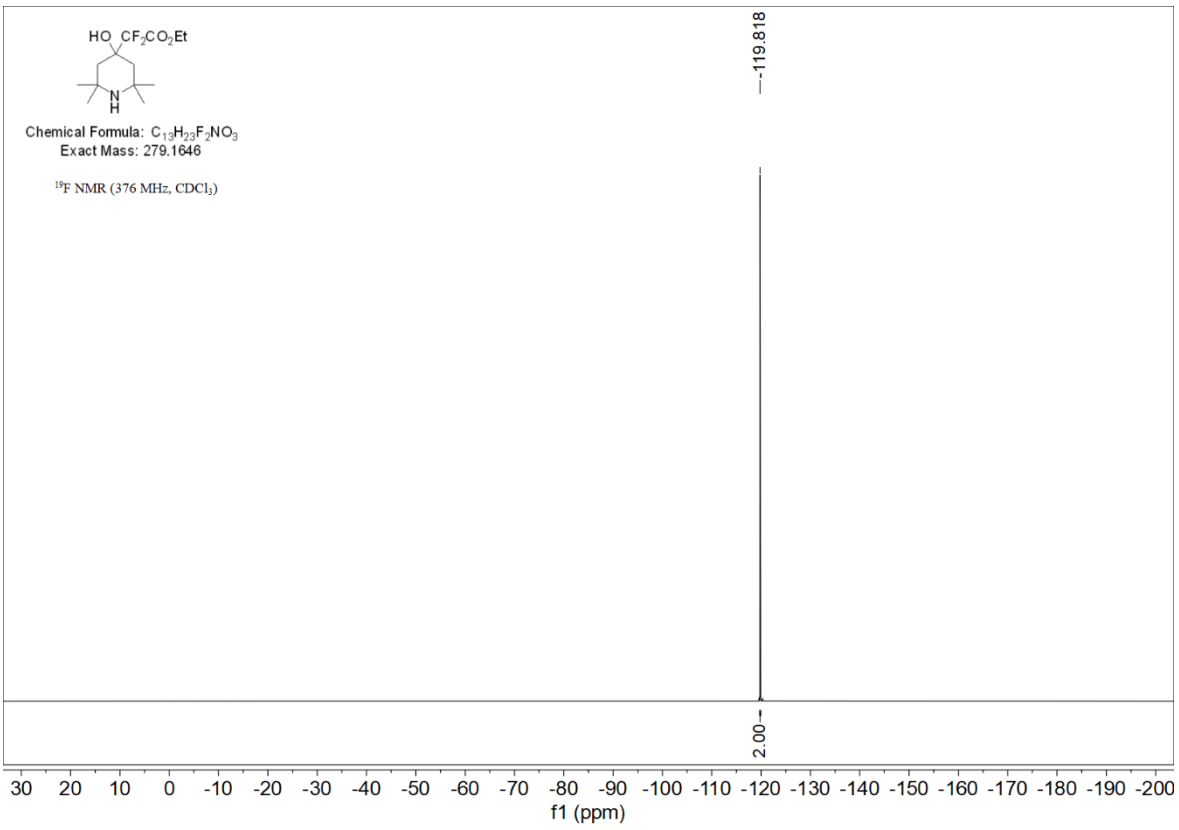
HO CF2CO2Et
Chemical Formula: C13H23F2NO3
Exact Mass: 279.1646
19F NMR (376 MHz, CDCl3)
-119.818
2.00
30 20 10 0 -10 -20 -30 -40 -50 -60 -70 -80 -90 -100 -110 -120 -130 -140 -150 -160 -170 -180 -190 -200
f1 (ppm)

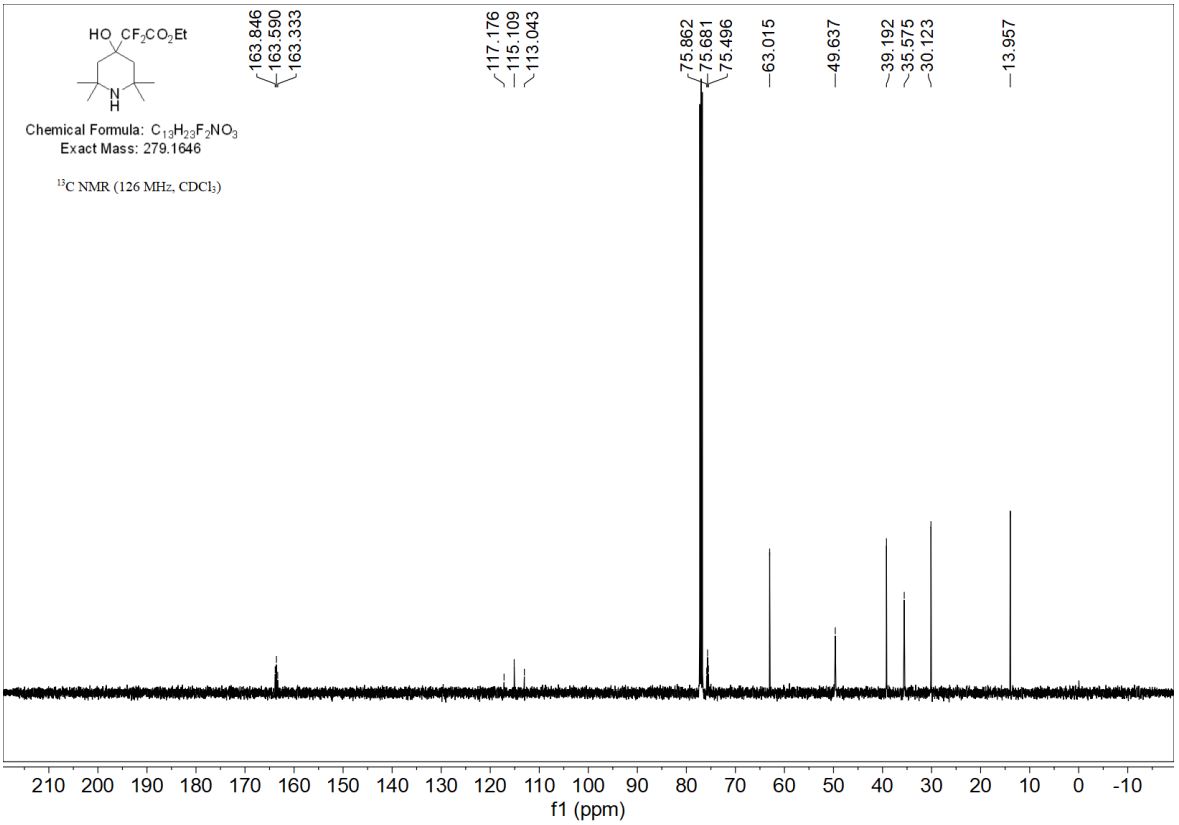
HO CF2CO2Et
Chemical Formula: C13H23F2NO3
Exact Mass: 279.1646
13C NMR (126 MHz, CDCl3)
163.846
163.590
163.333
117.176
115.109
113.043
75.862
75.681
75.496
63.015
49.637
39.192
35.575
30.123
13.957
210 200 190 180 170 160 150 140 130 120 110 100 90 80 70 60 50 40 30 20 10 0 -10
f1 (ppm)

Ethyl 2-(4-hydroxy-2,2,6,6-tetramethylpiperidin-4-yl)-acetate (H3).

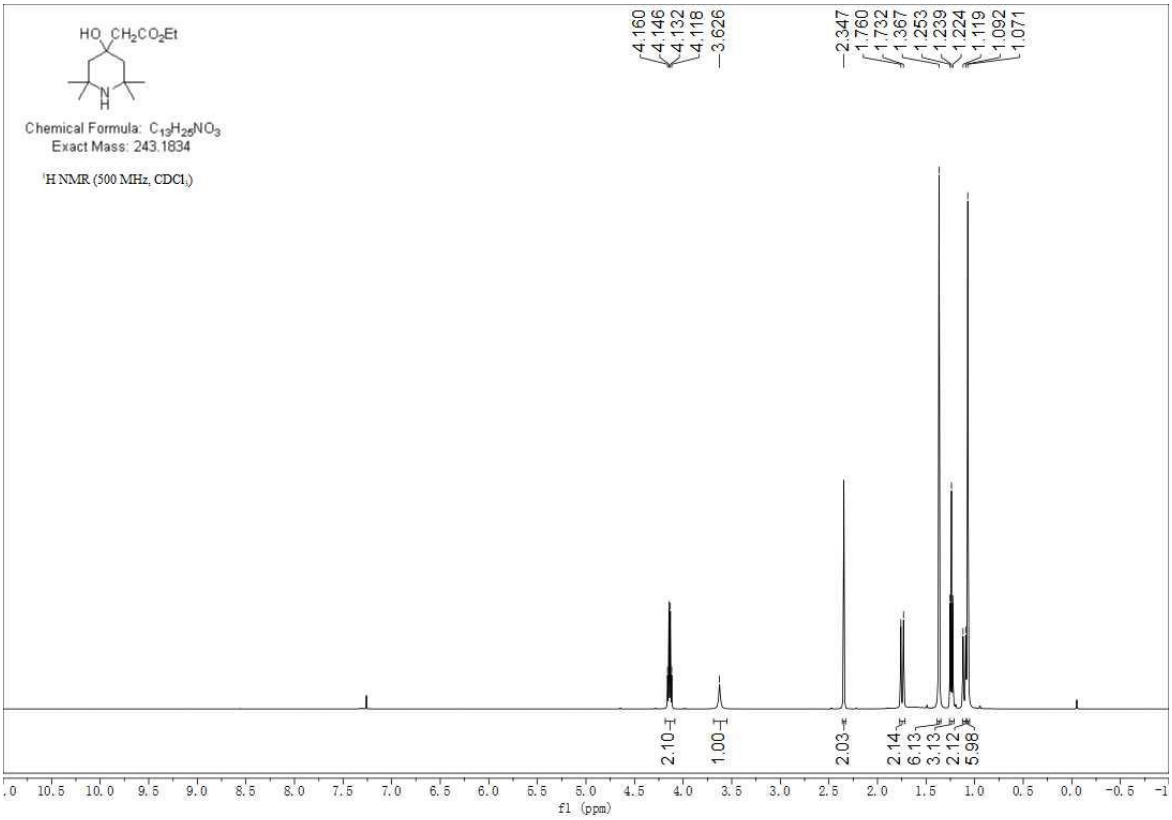

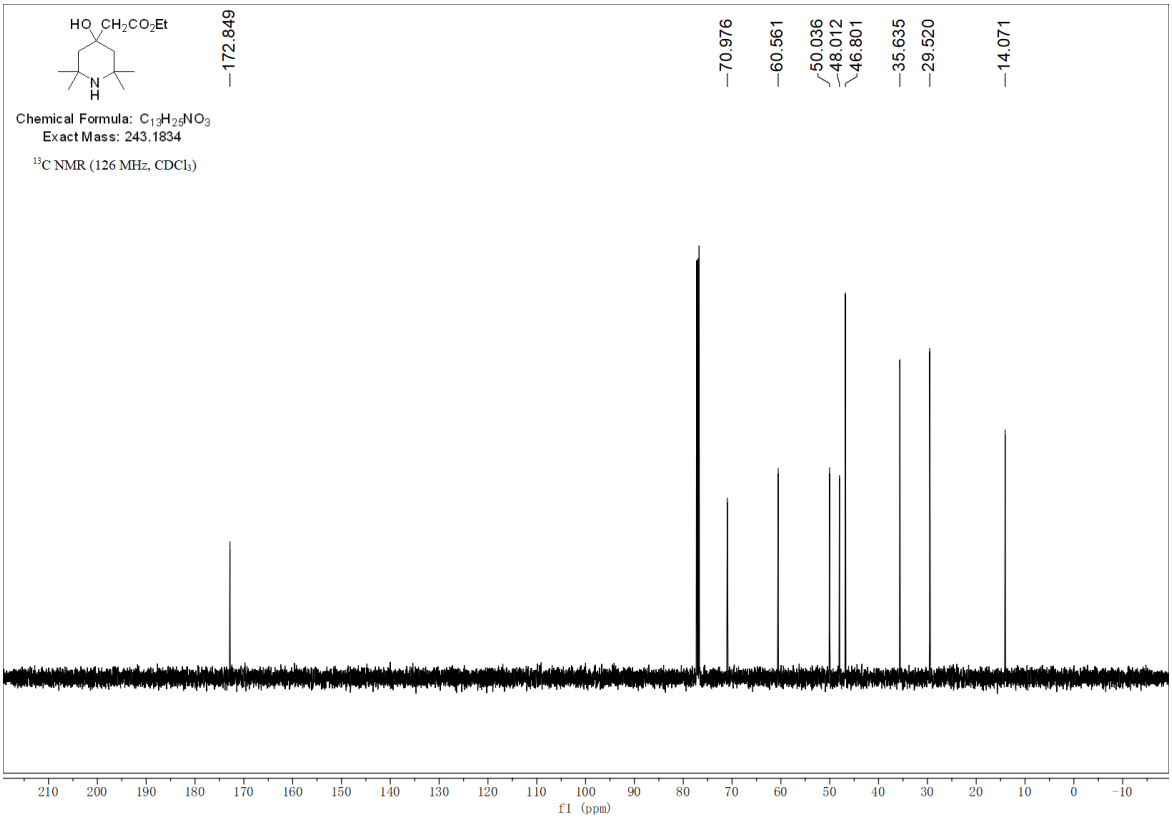

Ethyl 2-(4-hydroxy-2,2,6,6-tetramethylpiperidin-1-oxyl-4-yl)-2,2-difluoroacetate (4a).

NOTE: Compound **4a** was reduced by phenylhydrazine for NMR test.

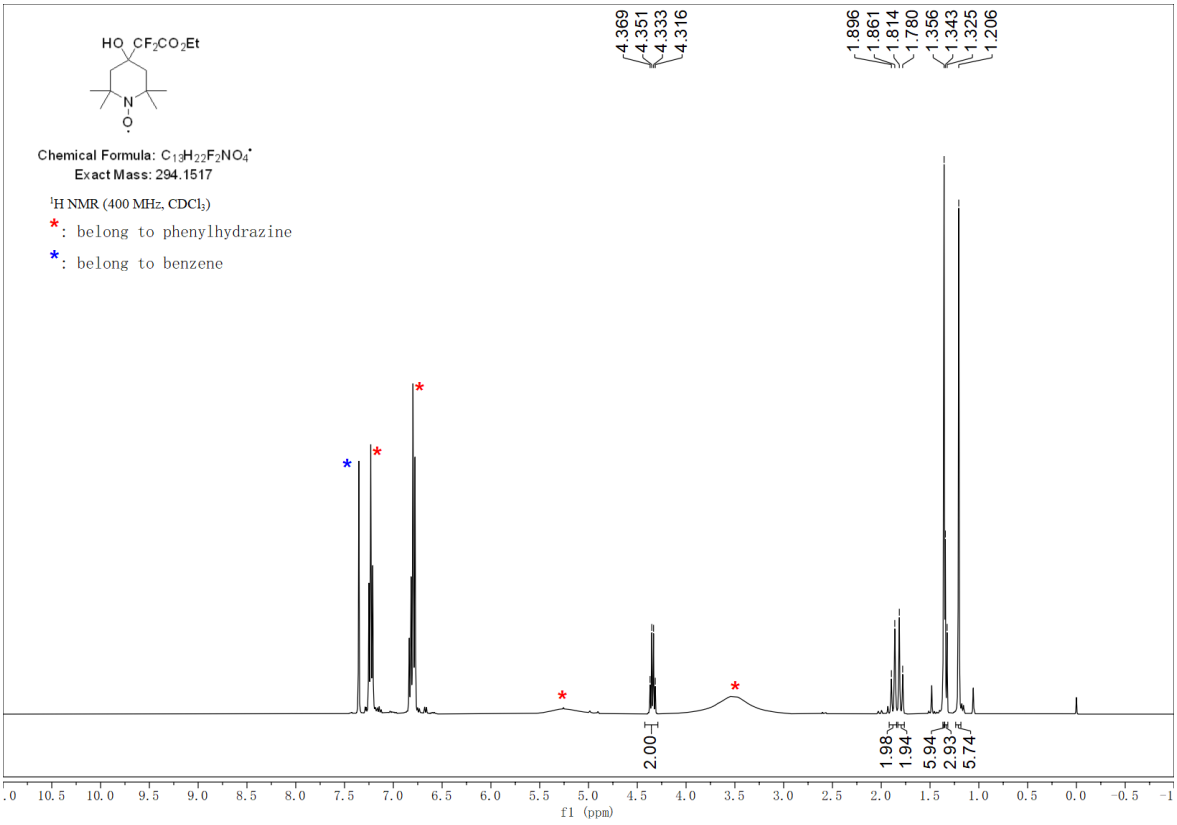

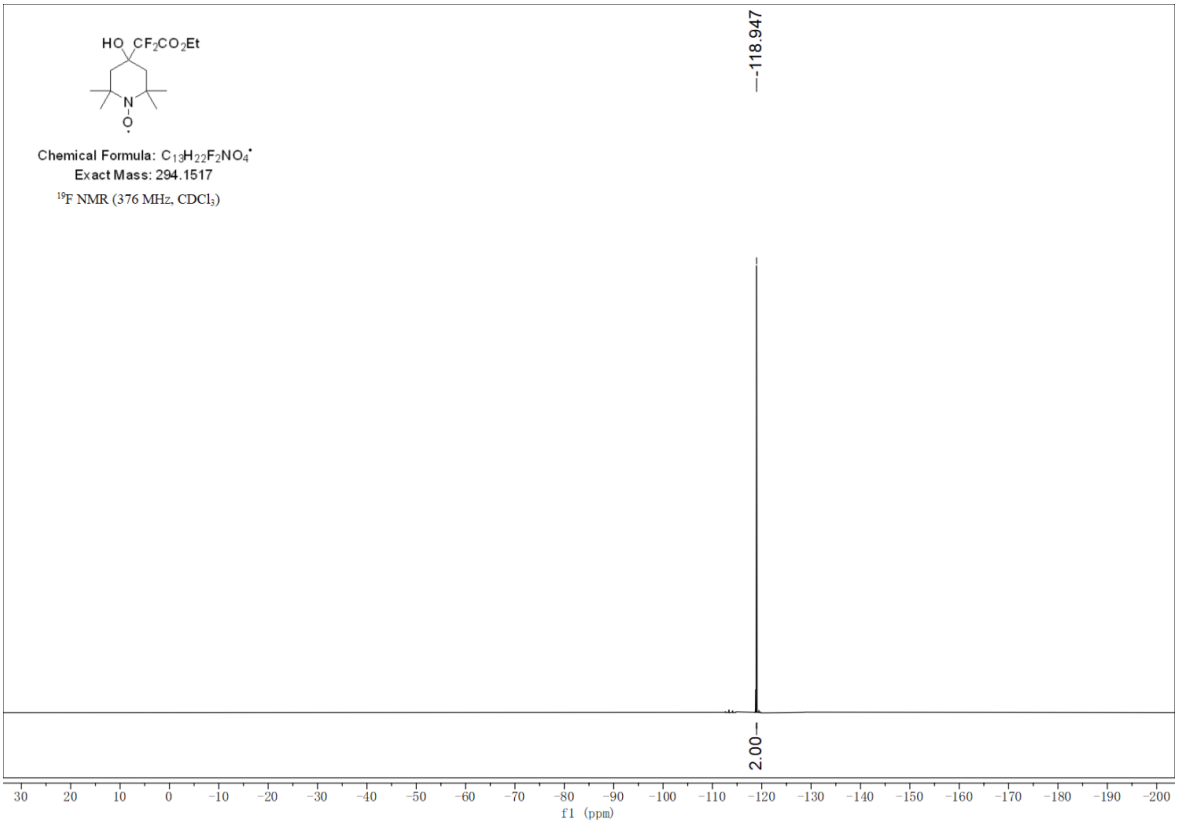

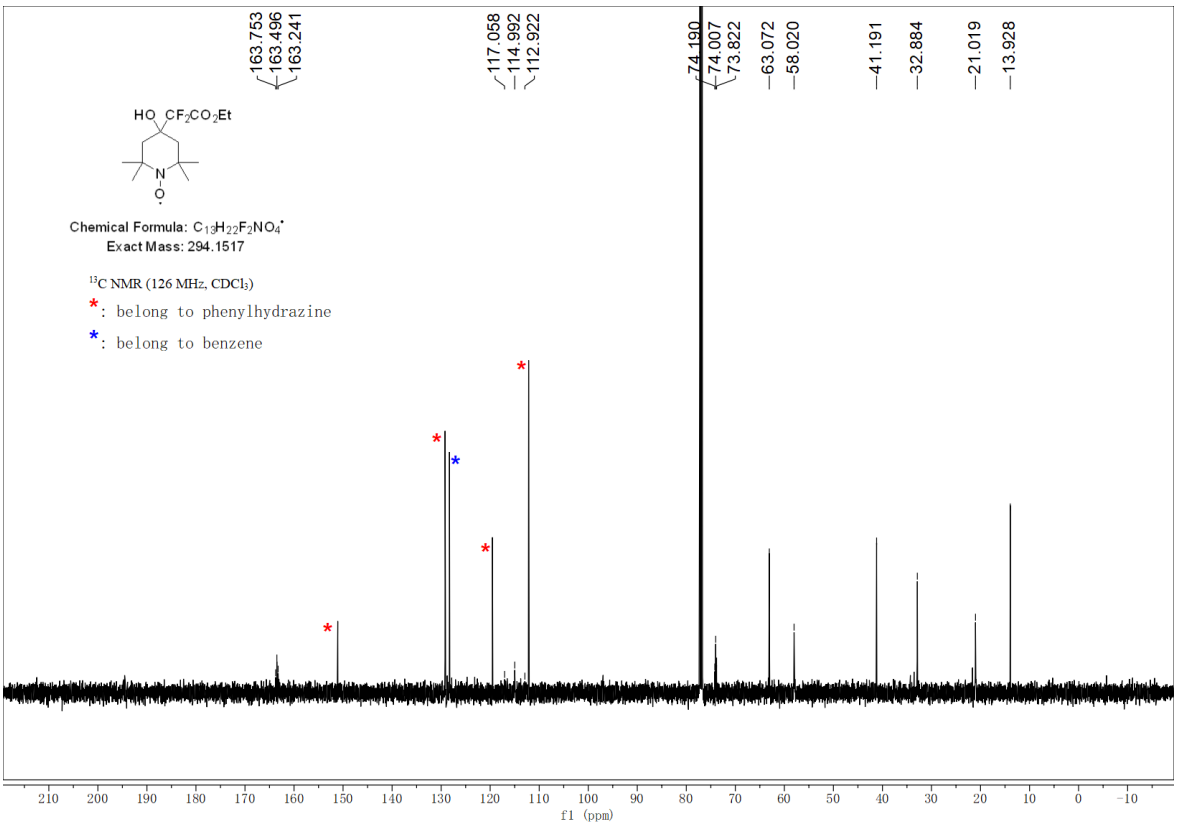

Ethyl 2-(4-hydroxy-2,2,6,6-tetramethylpiperidin-1-oxyl-4-yl)-acetate (4b).

NOTE: Compound **4b** was reduced by phenylhydrazine for NMR test.

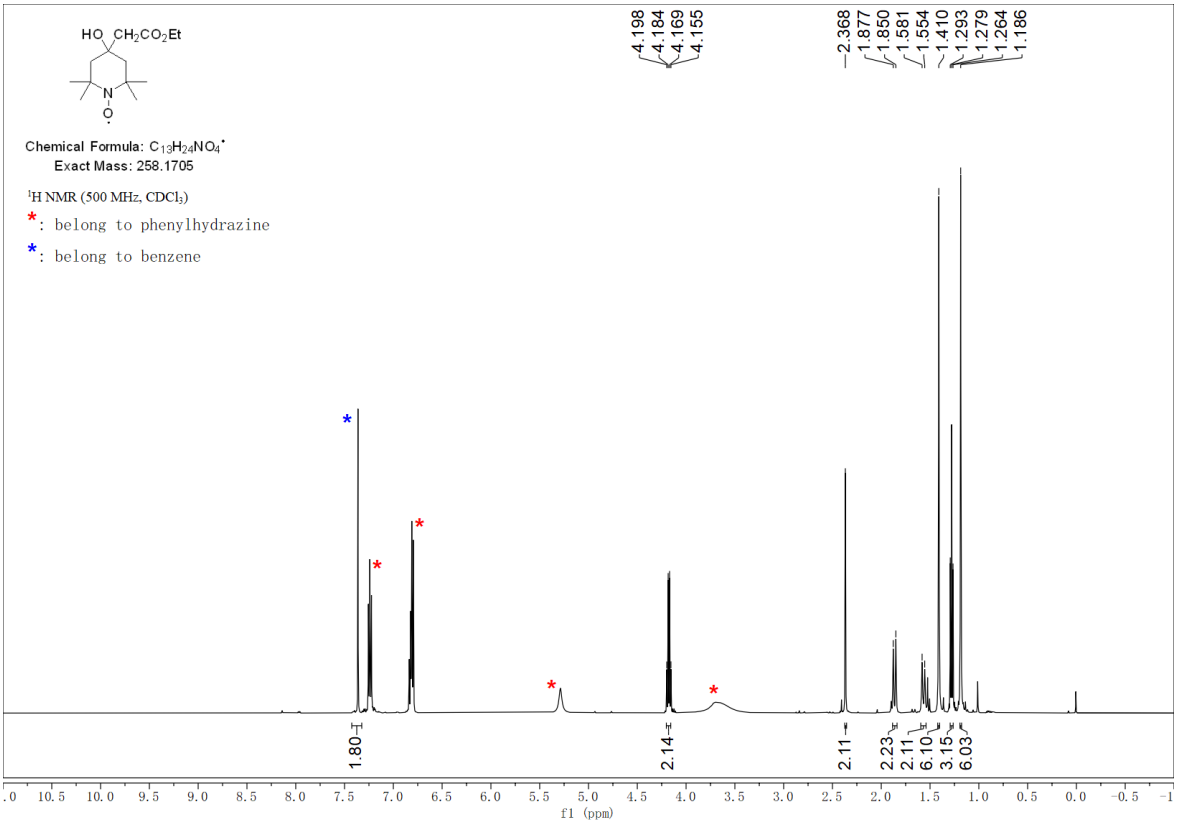

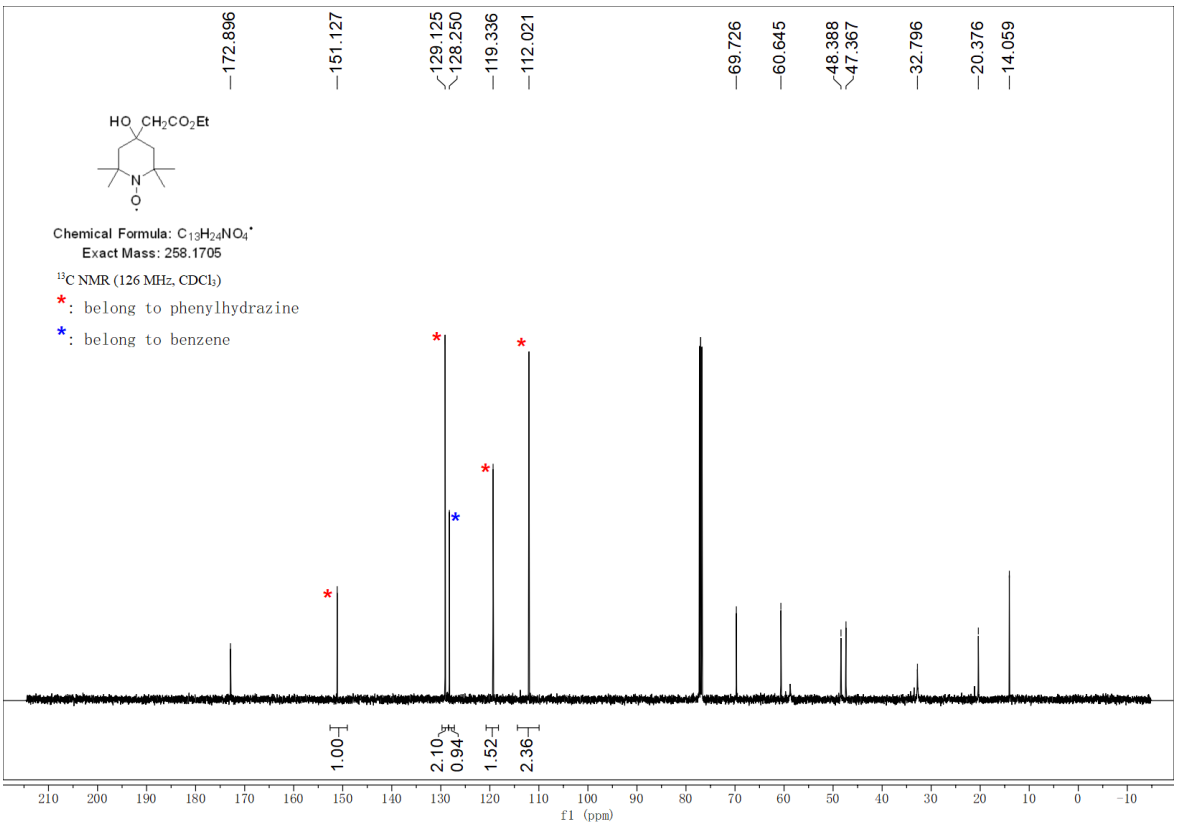

Sodium 2-(4-hydroxy-2,2,6,6-tetramethylpiperidin-1-oxyl-4-yl)-2,2-difluoroacetate (DFTEMPO).

NOTE: Compound **DFTEMPO** was reduced by phenylhydrazine for NMR test.

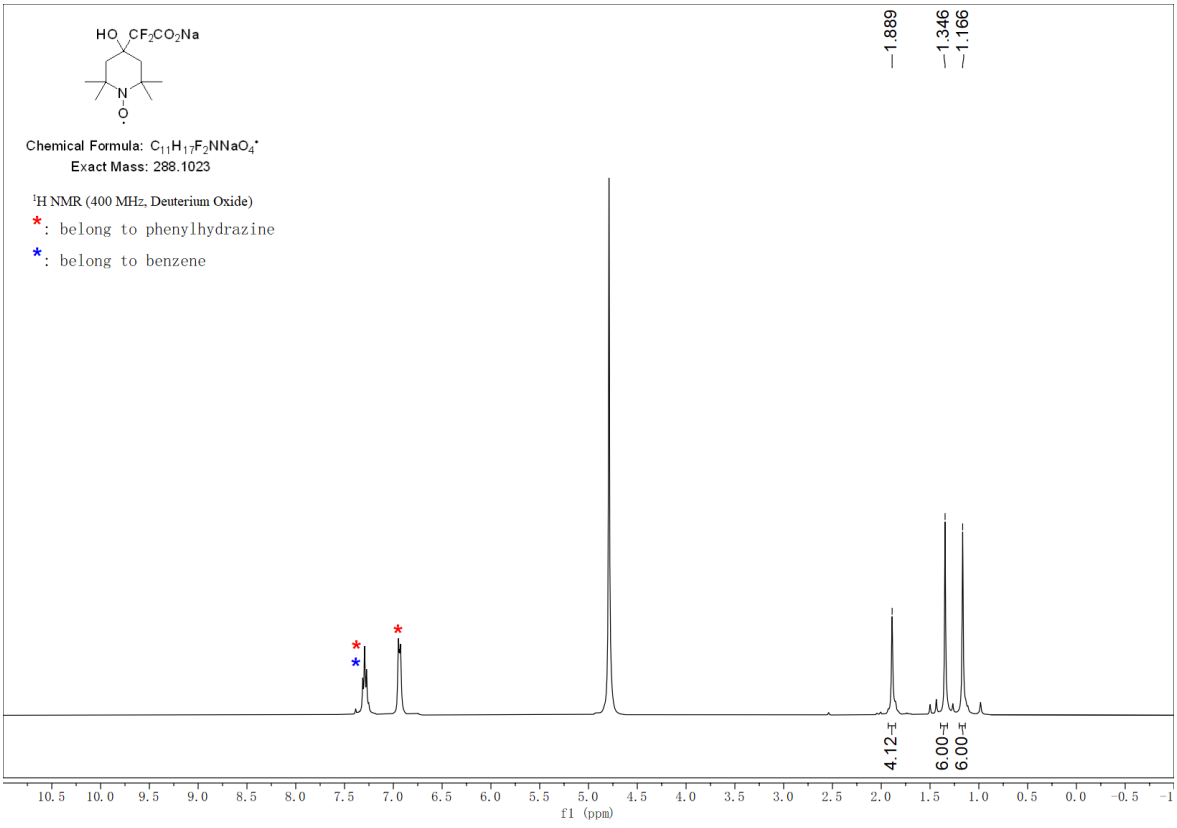

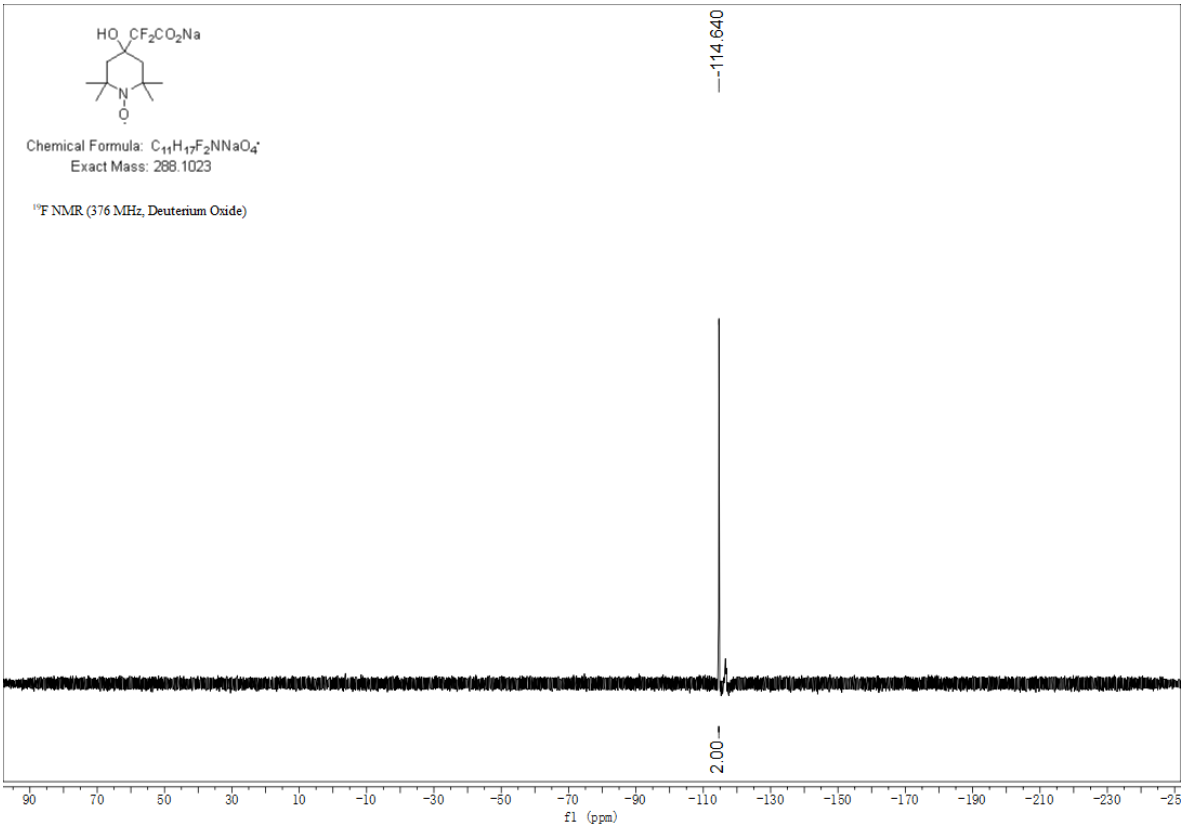

Sodium 2-(4-hydroxy-2,2,6,6-tetramethylpiperidin-1-oxyl-4-yl)-acetate (NFTEMPO).

NOTE: Compound **NFTEMPO** was reduced by phenylhydrazine for NMR test.

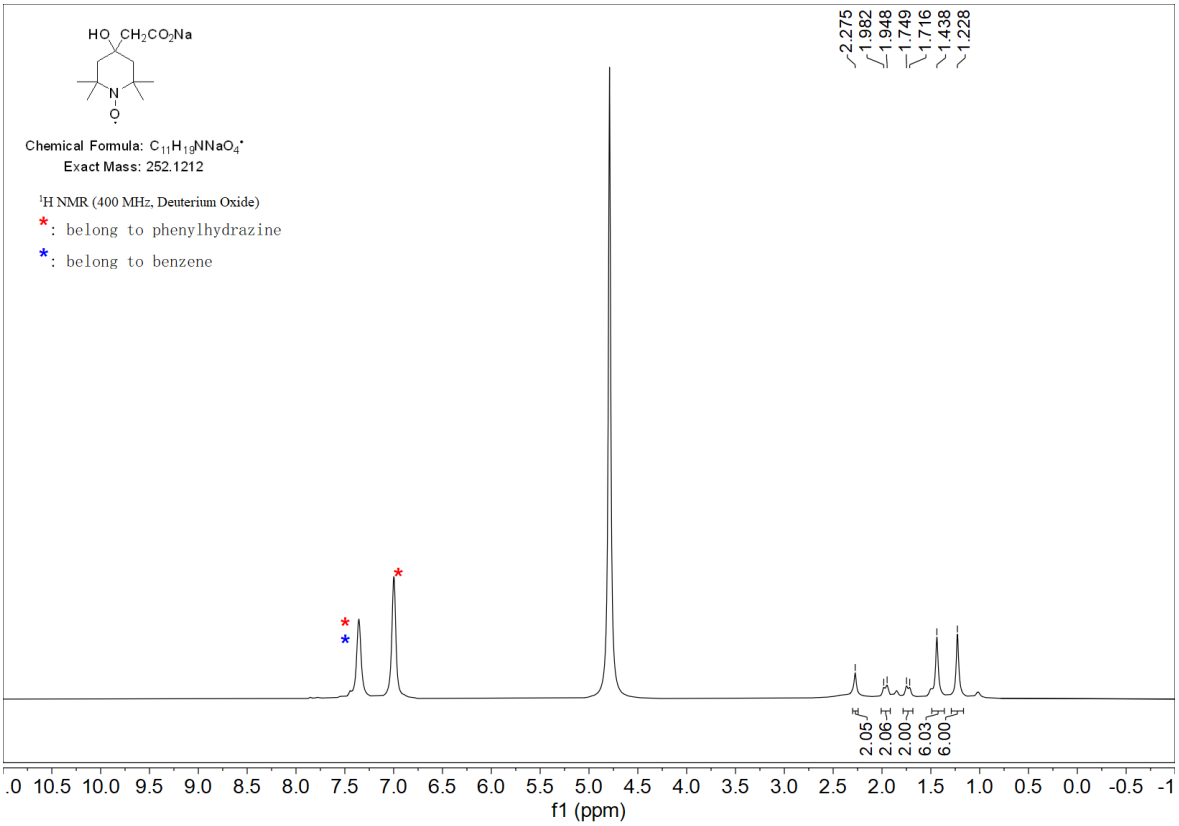

6. References

1. A. Orita, M. G. Verde, M. Sakai and Y. S. Meng, *J. Power Sources*, 2016, **321**, 126–134.
2. J. Winsberg, C. Stolze, A. Schwenke, S. Muench, M. D. Hager and U. S. Schubert, *ACS Energy Lett.*, 2017, **2**, 411–416.
3. Z. Chang, D. Henkensmeier and R. Chen, *ChemSusChem*, 2017, **10**, 3193–3197.
4. H. Fan, B. Hu, H. Li, M. Ravivarma, Y. Feng and J. Song, *Angew. Chem. Int. Ed.*, 2022, **61**, e202115908.
5. T. Janoschka, N. Martin, M. D. Hager and U. S. Schubert, *Angew. Chem. Int. Ed.*, 2016, **55**, 14427–14430.
6. B. Liu, C. W. Tang, H. Jiang, G. Jia and T. Zhao, *ACS Sustain. Chem. Eng.*, 2021, **9**, 6258–6265.
7. Y. H. Liu, M. A. Goulet, L. C. Tong, Y. Z. Liu, Y. L. Ji, L. Wu, R. G. Gordon, M. J. Aziz, Z. J. Yang and T. W. Xu, *Chem*, 2019, **5**, 1861–1870.
8. M. Gao, M. Salla, Y. Song and Q. Wang, *Angew. Chem. Int. Ed.*, 2022, **61**, e202208223; *Angew. Chem.*, 2022, **134**, e202208223.
9. S. Hu, L. Wang, X. Yuan, Z. Xiang, M. Huang, P. Luo, Y. Liu, Z. Fu and Z. Liang, *Energy Mater. Adv.*, 2021, **2021**, 9795237.
10. W. Zhou, W. Liu, M. Qin, Z. Chen, J. Xu, J. Cao and J. Li, *RSC Adv.*, 2020, **10**, 21839–21844.